Structures 82 (2025) 110734

Contents lists available at ScienceDirect

Structures

journal homepage: www.elsevier.com/locate/structures

Shear strengthening of sub-standard reinforced concrete beams with CFRP: Influence of fiber areal weight, wrap scheme and concrete strength

Deniz Sarı Alav [a], Yusuf Uysal [b], Ceyhun Aksoylu [c], Musa Hakan Arslan [c,*]

[a] Dursunbey Vocational School, Department of Construction, Balıkesir University, Balıkesir 10800, Türkiye
[b] Engineering Faculty, Department of Civil Engineering, Çanakkale Onsekiz Mart University, Çanakkale 17020, Turkiye
[c] Faculty of Engineering and Natural Sciences, Department of Civil Engineering, Konya Technical University, Konya 42250, Turkiye

ARTICLE INFO

Keywords:
CFRP strengthening
Wrap configuration
Experimental study
Concrete strength
Reinforced concrete beams

ABSTRACT

This study investigates the effectiveness of carbon fiber-reinforced polymer (CFRP) in enhancing the performance of reinforced concrete beams with insufficient shear reinforcement-a common issue in existing low- and high-strength reinforced concrete buildings. A total of 35 one-third scale beams were tested under four-point bending, considering varying concrete strengths (5–70 MPa), CFRP areal weights (300 and 900 g/m^2), and wrapping configurations (full (F), U-shaped (U), and side (S)). Key parameters such as load–displacement behavior, energy dissipation, ductility, and stiffness were analyzed in detail. The results demonstrated that CFRP strengthening increased shear capacity by up to 154 % in low-strength concrete (5–20 MPa), while the improvement was limited to 47.2 % in high-strength concrete. Failure modes were significantly influenced by wrapping type: full wrapping led to a 90 % shift from shear to flexural failure, whereas U-shaped and side wrapping achieved only 40 % and 10 % conversion, respectively. Full wrapping also yielded the highest gains in energy dissipation and ductility, while side wrapping alone was largely ineffective. Interestingly, increasing CFRP areal weight did not result in proportional performance gains; in many cases, the 300 g/m^2 application outperformed the 900 g/m^2 variant. This suggests that poor interfacial bonding and inadequate epoxy impregnation may hinder the effectiveness of higher areal weight configurations. In conclusion, concrete strength, wrapping type, and CFRP areal weight must be considered collectively in shear strengthening strategies. Among these, full wrapping offers the most consistent and reliable improvements in shear capacity, ductility. and energy dissipation.

1. Introduction

Structural elements are expected to exhibit adequate strength, rigidity, and ductility under the vertical and horizontal loads to which they will be subjected throughout the lifespan of structures. To ensure structural safety, not only must new structures be designed in accordance with codes, but existing structures must also be evaluated against both vertical and horizontal loads and their performance improved. Therefore, the topic of structural strengthening has received significant attention in both academic and applied engineering fields in recent years. Recent studies [1,2] have also emphasized that beyond ensuring sufficient strength. the resilience and post-earthquake recovery capacity of structural systems should be considered as key performance indicators. In particular research focusing on composite moment frames with slender concrete-filled steel tube (CFT) columns has demonstrated the effectiveness of connection behavior in improving overall seismic performance and highlighted the growing importance of resilience-based evaluation approaches [3].

Strengthening applications are used to increase the strength rigidity and ductility of existing structural elements [4]. In this context it is of great importance that the chosen method both achieves the desired effect and is practical (and economical) in terms of application. While the enlargement of reinforced concrete sections is commonly preferred for vertical load-bearing elements such as columns [5,6], lighter and more efficient solutions are favored for horizontal elements like beams to avoid volumetric interventions. In this direction, Fiber Reinforced Polymer (FRP) composites have been among the prominent materials in the strengthening of beam elements for approximately the last 30 years [7,8]. Different types of fibers such as glass [9,10], carbon [11], basalt [12], and aramid [13] are used in FRP systems; epoxy, polyester, vinyl

* Corresponding author.
E-mail address: mharslan@ktun.edu.tr (M.H. Arslan).

https://doi.org/10.1016/j.istruc.2025.110734
Received 12 October 2025; Received in revised form 14 November 2025; Accepted 18 November 2025
Available online 26 November 2025

ester or phenolic resins are preferred as the binding matrix materials [14,15].

Carbon FRP (CFRP) composites, in particular, are widely used in structural engineering applications thanks to their superior mechanical and physical properties. Thanks to their advantages such as high strength-to-weight ratio, high modulus of elasticity, and low specific gravity, CFRPs offer effective results in many structural strengthening applications. These fabrics, composed of woven carbon fibers, integrate with the resin matrix to form a composite structure, providing both high load-bearing capacity and resistance to environmental influences. The fibers offer high tensile strength, stiffness, and fatigue resistance, while the resin matrix provides load transfer between the fibers and protects the material against external factors such as moisture, chemical influences, and ultraviolet radiation. This resulting composite structure offers a significant alternative, particularly for strengthening structural elements with insufficient shear, flexural, and axial load capacity [16]. Beyond their contribution to conventional strengthening objectives, the use of CFRP materials has also become increasingly relevant within the framework of modern seismic design philosophies. In recent years, seismic-resilient design frameworks have evolved to assess not only the preservation of structural integrity but also the continuity of post-earthquake performance and rapid recovery capacity [17,18]. In this context, CFRP-based shear strengthening contributes to resilience-oriented design objectives by enhancing the energy dissipation capacity, ductility, and reusability potential of structures [3], while soil–structure interaction may also influence the deformation response of strengthened members [19,20].

Parameters such as fiber orientation, placement, length, and application method directly affect the mechanical performance of FRP systems. With appropriate placement strategies, it is possible to achieve the targeted strength and ductility criteria [21]. In this respect, FRP reinforcement applications offer both design flexibility and, thanks to the ease of on-site application, provide significant performance improvements in existing structures with minimal intervention [22]. Numerous studies exist in the literature on strengthening beams with insufficient shear capacity with CFRP. Studies examining the wrapping type [23–26] have shown that F-type wrapping contributes more to the failure mode, ductility, and load-carrying capacity of the beam compared to U- and side wrapping (S) types. Another study [27] has shown that CFRP contributes to the capacity of stirrups and tension reinforcement depending on the application method. Studies evaluating the effect of strip spacing on U-shaped wrappings [28–30] have reported that strip spacing greater than 60 mm does not provide any additional performance improvement; however, reducing the spacing delays pullout behavior, increasing load-carrying capacity, shear strength, and ductility. In studies indicating that the shear strength of the beam is improved with increasing CFRP strip width [31,32], it has been emphasized that this effect depends more on the strip spacing rather than the strip width [33]. In addition, the effects of the number of CFRP layers [34–36], the fiber ratio [37,38] and the application angle of the effective CFRP strips [39–43] on the beam behavior have been discussed in detail in the literature.

One of the most common problems encountered in CFRP applications, debonding behavior, occurs when effective load transfer between the fiber and the matrix cannot be achieved. For fibers to participate effectively in the load-carrying process, sufficient adhesion is required for load transfer from the matrix to the fiber. In the case of debonding, since no chemical bond is formed between the fiber and the matrix, load transfer occurs only through shear effects, which are ineffective when sufficient adhesion conditions are not met. Applications such as the use of mechanical anchors have been reported in the literature to reduce this problem [44–50]. Additionally, increasing the proportion of fine material in concrete [51,52] is among the methods aimed at improving the adhesion between CFRP and concrete. In addition, defects such as delamination and insufficient epoxy absorption in CFRP applications are also among the important factors that negatively affect beam performance. Delamination occurs when proper adhesion between multiple CFRP layers is not achieved and restricts load transfer, preventing the expected capacity increase. Similarly, insufficient epoxy resin absorption or failure to completely coat the fibers weakens the adhesion between CFRP and concrete and can prevent premature fiber engagement, especially in high-weight applications. Such application defects increase the risk of debonding and limit the ductility and energy dissipation capacity of beams. In the literature, methods such as increasing surface roughness, determining the appropriate resin amount, and applying mechanical anchors are recommended to minimize these problems [53,54].

Studies in the literature have also evaluated other parameters affecting the structural performance of FRP-strengthened beams. For example, the shear span [55–59], beam size [60], epoxy type [61,62], number of wraps [63,64], wrapping type [65] and shear span to depth ratio (a_v/d) [58,59] have been tested for the effects of variables on load-carrying capacity and durability. Numerous studies in the literature have demonstrated that CFRP strengthening increases shear capacity [44,48,55,56,65]. Furthermore, the CFRP bonding method, number of layers, type of first layer, strip angle, and strip spacing have been identified as important parameters affecting beam performance [33,35,36]. However, experimental studies on elements with varying concrete strengths indicated that, for very low concrete strengths, CFRP tended to peel off prematurely from the concrete surface, failing to provide the expected contribution, whereas at high concrete strengths (C50 and above), the effectiveness of the strengthening decreased [66–71].

1.1. Research gaps in the literature

In countries such as Turkey, where a substantial portion of the existing building stock suffers from inadequate load-bearing capacity, CFRP strengthening techniques are widely employed. Despite their prevalence, both the existing literature and current design codes offer limited comprehensive guidance on these practices. Key issues remain unresolved, including the effectiveness of CFRP applications in low-strength concrete elements, the need to adapt wrapping configurations based on concrete strength, and the influence of CFRP areal weight on performance. The Turkish Building Earthquake Code (TBEC 2018) [64] lacks detailed provisions regarding critical parameters such as concrete properties (strength, composition, cross-sectional dimensions), reinforcement detailing (spacing, diameter, placement). CFRP fabric characteristics (areal weight, number of layers, spacing, overlap length, and wrapping configuration), and adhesive specifications. Moreover, the code permits only F-type strengthening, with no reference to U-type or side (S-type) applications, which limits design flexibility and practical implementation.

1.2. Scope and significance of the study

Since the use of carbon fiber-reinforced polymer (CFRP) materials in structural strengthening is relatively recent compared to traditional methods, their interaction with existing reinforced concrete elements—particularly in relation to concrete strength—has not yet been fully clarified. In addition to gaps in the literature, current design and strengthening codes also fall short in addressing these issues. For instance, while the Turkish Building Earthquake Code (TBEC 2018) [72] mandates a minimum concrete class of C25 for new constructions, it lacks detailed guidance on the procedures and specifications for strengthening existing structures using CFRP. International standards such as ACI 440.2R-17 [73], FIB-2010 [74], and CNR-DT200–2013 [75] permit the use of F-type (full), U-type, and S-type (side) wrapping configurations, and define threshold values for minimum compressive and tensile strengths of concrete. Notably, ACI 440.2R-17 recommends using only F-type wrapping for concrete with compressive strength below 17 MPa. Against this backdrop, the present study experimentally investigates the effects of CFRP strengthening on the shear capacity and

damage behavior of beams with concrete strengths ranging from 5 to 70 MPa. Three wrapping configurations (F – full wrap, U – U-wrap, and S – side wrap) and two CFRP areal weights (300 and 900 g/m^2) were considered. While concrete strengths up to 70 MPa exceed those commonly used in typical building stock (generally 5–30 MPa), such high-strength specimens are included to extend the applicability of the findings to special cases such as high-performance structures or infrastructure elements, and to evaluate the behavior of CFRP strengthening across a broad range of concrete strengths. This allows for a more comprehensive understanding of the interaction mechanisms between CFRP and concrete, which can inform both conventional and specialized applications. This approach enables a comprehensive evaluation of how concrete strength, wrapping type, and CFRP areal weight influence the structural performance of reinforced concrete beams.

2. Experimental study

2.1. Test matrix

In this study, a total of 35 reinforced concrete beam specimens designed to have insufficient shear strength were prepared and tested in a laboratory environment. Five of the specimens were designated as the reference group without any sterngthening. while the remaining 30 beams were strengthened using different wrapping configurations and CFRP properties. In the experimental program, the variable parameters were concrete compressive strength, wrapping type, and areal weight of the CFRP strips. Beams were produced in five different targeted concrete compressive strength ranges (5–10 MPa, 10–20 MPa, 30–40 MPa, 50–60 MPa, and 60–70 MPa), and seven specimens were prepared for each range. Thus, the effects of both concrete strength and CFRP application parameters on shear behavior were systematically evaluated (Table 1).

Three different wrap configurations, F, U, and S, were used in CFRP reinforcement applications. For each wrap type, unidirectional (±90°) CFRP strips with areal weights of 300 g/m^2 and 900 g/m^2 were selected. A total of seven specimens were designed for each concrete strength class: one unreinforced reference specimen and six different strengthening specimens (3 wrap types × 2 weights). Specimen coding is systematically presented in Table 1 according to the targeted concrete compressive strength range, wrap type, and areal weight of CFRP parameters. For example, specimen BF1–1 was produced with concrete having a compressive strength of 5–10 MPa and strengthened with 300 g/m^2 CFRP using type F wrap. Similarly, specimen BF1–2 was prepared with the same concrete strength and wrap type, but strengthened with 900 g/m^2 CFRP.

2.2. Details of specimens

All specimens were designed to be 1/3 the geometric scale of the actual prototypes, 1000 mm long, 150 mm high, and 100 mm wide, and were manufactured using standard molds. While material properties could not be directly scaled, the longitudinal and transverse steel

Table 1
Test matrix.

Specimen Code	Targeted Concrete Strength (MPa)	CFRP Areal Weight (g/m^2)		Strengthening Type			
		300	900	reference	F	U	S
							
B1–0	5–10			√			
BF1–1	5–10	√			√		
BF1–2	5–10		√		√		
BU1–1	5–10	√				√	
BU1–2	5–10		√			√	
BS1–1	5–10	√					√
BS1–2	5–10		√				√
B2–0	10–20			√			
BF2–1	10–20	√			√		
BF2–2	10–20		√		√		
BU2–1	10–20	√				√	
BU2–2	10–20		√			√	
BS2–1	10–20	√					√
BS2–2	10–20		√				√
B3–0	30–40			√			
BF3–1	30–40	√			√		
BF3–2	30–40		√		√		
BU3–1	30–40	√				√	
BU3–2	30–40		√			√	
BS3–1	30–40	√					√
BS3–2	30–40		√				√
B4–0	50–60			√			
BF4–1	50–60	√			√		
BF4–2	50–60		√		√		
BU4–1	50–60	√				√	
BU4–2	50–60		√			√	
BS4–1	50–60	√					√
BS4–2	50–60		√				√
B5–0	60–70			√			
BF5–1	60–70	√			√		
BF5–2	60–70		√		√		
BU5–1	60–70	√				√	
BU5–2	60–70		√			√	
BS5–1	60–70	√					√
BS5–2	60–70		√				√

reinforcement ratios and concrete compressive strengths were selected to maintain proportional stress and strain distributions, ensuring approximate kinematic similarity in bending and shear behavior. The tests were conducted under quasi-static loading conditions, so dynamic similarity was not a governing factor in this study. These considerations allow the experimental results to be meaningfully related to full-scale structural behavior. Two Ø8 diameter rebars were placed longitudinally in the upper section of the beams, and two Ø10 diameter rebars were placed in the lower section. The reinforcement ratios were selected to exceed the minimum reinforcement limits specified in the TS 500–2000 [76] regulation. The beams were aimed to have a higher flexural capacity than their shear capacity, thus ensuring that the specimens would fail primarily due to shear damage. Accordingly, the Ø6 diameter stirrups used along the shear span were spaced at sparse intervals (320 mm), well above the regulation limits. On the other hand, in the middle section, where bending is more effective, and around the support, the Ø6 diameter stirrups were spaced closely at 50 mm intervals to limit potential damage and prevent local crushing. Additionally, the cover distance from the center of the tensile reinforcement to the outer surface of the concrete was determined as 35 mm, and plastic spacers were used to maintain this distance and to ensure the reinforcement was fixed in the correct position. The dimensioning and reinforcement arrangements of the beam specimens used in the experimental study are presented in Fig. 1.

2.3. Materials

Various building materials, including concrete mix, steel reinforcement, CFRP fabric, and epoxy-based adhesive, were used in the fabrication and strengthening of the specimens used in the experimental study. The mechanical and physical properties of these materials are presented in detail under the relevant subheadings.

2.3.1. Concrete

The concretes used in the test specimens were produced in both industrial facilities (30–40 MPa, 50–60 MPa, and 60–70 MPa) and under controlled laboratory conditions (5–10 MPa and 10–20 MPa) to represent different compressive strength ranges. Concrete mixes prepared in five different targeted concrete compressive strength ranges were produced in only one production cycle for each strength level, ensuring continuity and consistency in experimental comparisons.

The laboratory-prepared concrete mixes were prepared using the classic concrete components of water, cement, fine aggregate, and coarse aggregate. Additional chemical admixtures were used in mixes with target compressive strengths of 50–60 MPa and 60–70 MPa, while no admixtures were used in other ranges. As a binder. CEM IV/B (P) 32.5 R-SR type pozzolanic cement, resistant to sulfate effects, was used in concrete mixes with compressive strengths of 5–10 MPa and 10–20 MPa. For mixtures in the 30–40 MPa, 50–60 MPa, and 60–70 MPa ranges. CEM IV/B (P) 42.5 R-SR type cement was preferred. The material quantities corresponding to 1 m^3 of concrete in each mixture are presented in Table 2.

During the placement of fresh concrete in the molds, compaction was performed using mechanical vibration to minimize air voids and achieve a homogeneous internal structure. Three 150 × 150 × 150 mm cube samples and additional 150 mm/300 mm cylinder samples were prepared for each concrete class to determine mechanical properties. All compressive strength tests were conducted in accordance with EN 12390–3 [77]. The 28-day compressive strength results for different strength ranges and the data obtained from splitting tensile tests applied to cylinder samples are presented in Table 3, and images of the sample production and testing process are presented in Fig. 2.

2.3.2. Rebar

The beam specimens examined in the experimental study were manufactured using steel rebars of different diameters and properties. In the longitudinal reinforcement arrangement, two 10 mm diameter rebars were placed in the tension zone and two 8 mm diameter rebars were placed in the compression zone, 6 mm diameter ribbed stirrups were used as transverse reinforcement and were applied at regular intervals of 320 mm along the shear span of all beams. In the middle region, where shear stresses were assumed to be negligible, the stirrup spacing was increased to 50 mm to prevent local crushing that might occur under loading points. To prevent fractures in the support area, two stirrups were placed at 30 mm intervals. The mechanical properties of all steel rebars used were determined through tensile tests conducted in accordance with EN ISO 15630–1 [78] and EN ISO 6892–1 [79]. Information on the mechanical properties of the reinforcement used in the beams is presented in Table 4.

2.3.3. CFRP fabric

In this study, CFRP fabric materials with two different areal weights were used to increase the shear strength of the beams. The CFRP fabrics used have areal weights of 300 g/m^2 and 900 g/m^2, and both are composed of unidirectional, high-tensile carbon fibers. The CFRP fabrics were placed in ±90° orientations and applied to the test beams by the wet lay-up method. The fabrics were cut to suit both the wrapping type

Table 2
Material constituents of concrete mix (1 m^3).

Material constituent	Target Concrete Compressive Strength (MPa)				
	5–10	10–20	30–40	50–60	60–70
Cement (kg)	307	285	432	325	301
Aggregate (15–22) (kg)	1008	1041	863	519	535
Aggregate (5–15) (kg)	-	-	-	546	497
Aggregate (0–5) (kg)	656	659	754	885	879
Water (kg)	309	285	251	153	185
Additive Material (kg)	-	-	-	3	3
Water/Cement Ratio (kg/kg)	1.01	1.00	0.58	0.47	0.61

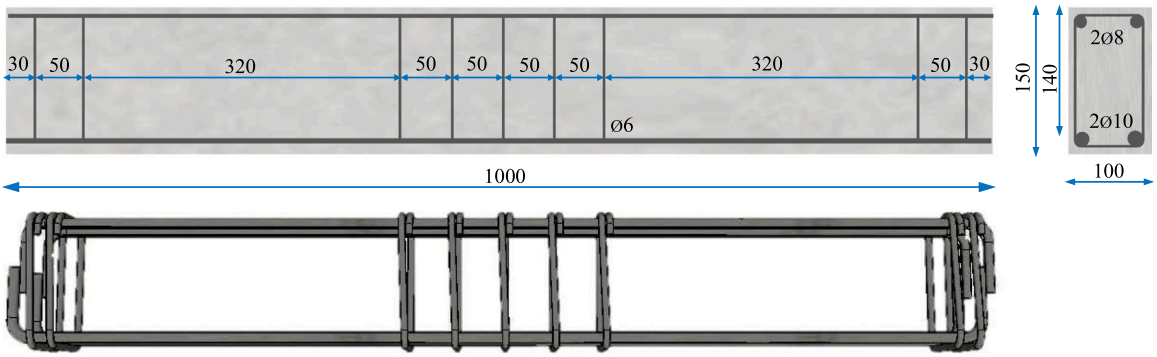

Fig. 1. Schematic representation of the geometric and reinforcement details of the beams used in the experimental study (cm).

Table 3
Compressive and tensile strengths of concrete.

Target compressive strength range (MPa)	Average concrete compressive strength (MPa)	Average concrete tensile strength (MPa)
5–10	6.71	0.91
10–20	16.04	1.49
30–40	37.86	3.25
50–60	52.00	3.57
60–70	63.88	3.75

and the beam dimensions. For both CFRP areal weights used, the minimum wrapping width of 30 mm, as recommended by Aksoylu [26] in the literature, was taken as the basis. Depending on the wrapping type, strips of 600 mm for F wrappings, 400 mm for U wrappings, and 150 mm for S wrappings were prepared. These dimensions were determined to fully cover the surface area where each wrapping type will be effective on the beam. The basic mechanical properties of the CFRP fabric material used are summarized in Table 5. The CFRP fabrics with areal weights of 300 g/m^2 and 900 g/m^2 used in the study are presented in Fig. 3.

2.3.4. Epoxy-based systems in CFRP strengthening

In FRP systems used in strengthening applications, the aim is for fiber materials to function as composites with polymer matrices. Properties of the polymer matrix, such as thermal stability, chemical resistance, and creep resistance, are critical to the long-term performance of the system. The three main resin types commonly used in composite production are polyester, epoxy, and vinyl ester, each with its own unique advantages. Polyester resins are among the most preferred matrix materials due to their affordability, light weight, and heat resistance, while epoxy resins offer superior mechanical properties along with low viscosity and low shrinkage. Vinyl ester resins, on the other hand, are particularly preferred in FRP rod production due to their high resistance to chemical attack. In this study, MapeWrap Primer 1 primer was used primarily during the surface preparation phase of applying CFRP fabrics to the concrete surface, MapeWrap 31, a high-performance epoxy-based adhesive, was used for bonding the CFRP fabrics. Both products are two-component and were prepared according to the manufacturer's recommended mixing ratios (3:1 for MapeWrap Primer 1, 4:1 for MapeWrap 31). The prepared mixtures were applied first as primers and then as adhesives, respectively. The basic mechanical and physical properties of the epoxies and their conditions of use are presented in Table 6.

2.4. Strengthening procedures

Before proceeding with CFRP strengthening of reinforced concrete beams with insufficient shear capacity, surface preparation was performed. Fig. 4 shows the application steps for reinforced concrete beam strengthening using the CFRP technique. First, the beam surfaces were ground to remove any weak cement grout. Surface defects such as voids and cracks that could hinder the application were identified and repaired with a suitable repair mortar. For beams undergoing F and U-type wrapping, corner rounding was performed with a mechanical grinding machine with a 30 mm radius to reduce stress concentrations in the corner areas and to prevent CFRP strips from breaking (Fig. 4(a)). The dust layer formed after grinding and corner rounding was removed using a compressor, and then the surfaces were washed with water to prepare them for application Fig. 4(b).

Following surface preparation, appropriate layout plans were drawn on the beams. numbered according to the wrapping type (F, U, S) and fabric type to be applied to each beam Fig. 4(c). The CFRP fabrics were cut to match the fiber orientations of the wrapping (Fig. 4(d and e)), Strips of 30 mm width and lengths of 600 mm for the F type, 400 mm for the U type, and 150 mm for the S type were prepared from the two different areal weights of fabric used, depending on the wrapping type. To prevent the fibers from spreading, taping was performed along the edges before cutting.

The surface primer mixture, which can be processed for approximately 90 min at + 23°C. was applied with a consumption of approximately 250–300 g/m^2. This primer mixture was applied to the concrete surface, ensuring no gaps were left, and the next step was carried out immediately (Fig. 4(f)). A two-component epoxy adhesive, mixed at the manufacturer's recommended 4:1 weight ratio, was applied to one side of the prepared CFRP strips. The adhesive-coated strips were carefully placed on the concrete surface, aligning the fiber orientation and wrapping type. To ensure complete adhesion of the fibers and prevent air pockets during application, the epoxy mixture was reapplied to the outer surface of the fabric to create a homogeneous layer. Particular attention was paid to ensuring no gaps were left between the CFRP and the concrete in the pre-beveled corner areas, particularly in the F and U

Table 4
Mechanical properties of rebars.

Nominal diameter (mm)	Surface deformation	Average yield strength (MPa)	Average ultimate tensile strength (MPa)	Remarks
10	Ribbed	445	558	Tension Bar
8	Ribbed	482	592	Compression Bar
6	Ribbed	488	712	Stirrup

Table 5
Mechanical properties of CFRP.

Property	CFRP Areal weight	
	900 g/m^2	300 g/m^2
Tensile Strength (GPa)	4.40	3.95
Elastic Modulus (MPa)	235	238
Rupture Strain (%)	1.87	1.60
Thickness (mm)	0.50	0.17

Fig. 2. Specimens prepared for compressive and splitting tests and the testing procedure.

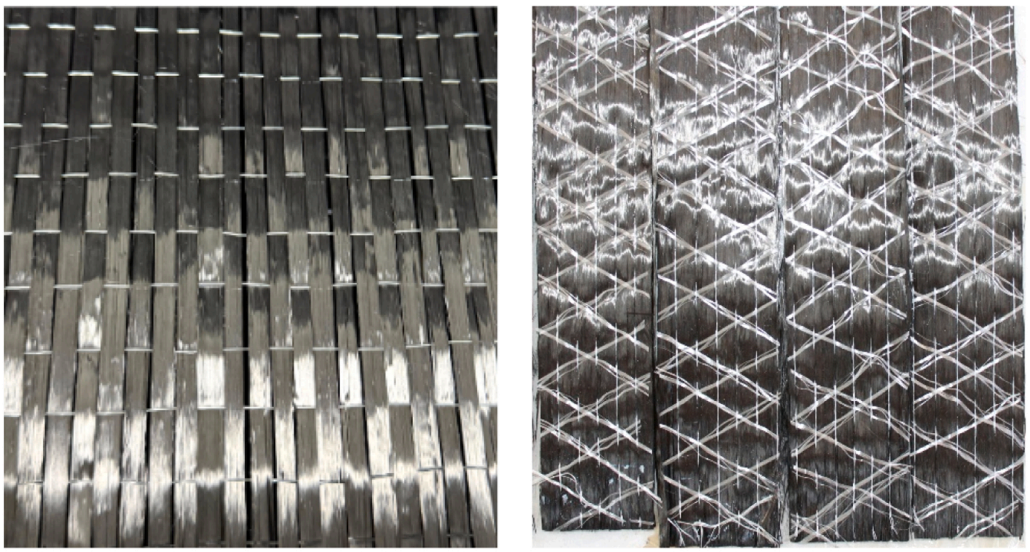

Fig. 3. CFRP fabrics with areal weights of 300 g/m² and 900 g/m².

Table 6
Properties and application conditions of the epoxy materials used.

Property	Component A	Component B	Component A	Component B
Consistency	Liquid	Liquid	Paste	Paste
Color	Transparent yellow	Transparent yellow	Dark yellow	Light yellow
Density (g/cm³)	1.12	1	1.34	1.25
Mixing ratio	3	1	3	1
Cure time:			4 h	
+ 10°C:	5–6 h			
+ 23°C:	3–4 h			
+ 30°C:	2–3 h			
Working time			40 min	
+ 10°C:	120 min			
+ 23°C:	90 min			
+ 30°C:	60 min			
Application temperature	+ 10°C to + 30°C		+ 5°C to + 30°C	
Full cure time	7 days		7 days	

type wraps. All applications were carried out in accordance with the manufacturer's specifications, adhering to the epoxy mixture's workability time of approximately 40 min at + 23°C and the recommended consumption amounts (1000–1100 g/m² for 300 g/m² fabrics and 1300–1400 g/m² for 900 g/m² fabrics).

The three wrapping configurations applied in the experiments exhibit different behaviors in terms of shear stress restraint in various directions and continuity of the wrapping. For each concrete strength, one reference specimen and six different CFRP configurations were designed to systematically evaluate the effect of wrapping types on shear strength. Schematic views of the reference and strengthened specimens are presented in Fig. 5.

2.5. Instrumentations and testing set-up

A four-point bending test was conducted to determine the flexural and shear behavior of beam specimens. A schematic representation of the test setup is presented in Fig. 7, Specimens were placed in the test setup with fixed supports, 50 mm inward from the beam ends. For the purpose of the test, the shear span to depth ratio was selected as $a_v/d = 350/140 = 2.5$ to ensure shear fracture in the specimens; accordingly, the shear span was determined as $a_v = 350$ mm. Loading was applied in 10 kN increments using a mechanically controlled hydraulic pump, and the loads were measured instantaneously with a 300 kN capacity load cell. The total applied load P was transmitted symmetrically to the beam as equal-magnitude forces P/2 from two points via the loading beam. The distance between these two single load points was set at 200 mm. Short pauses were performed after each load increment to monitor crack formation and propagation during loading. Two potentiometers, 200 mm apart, were placed at the mid-span of the beams, in the area where shear is assumed to be minimal and bending moment constant. These potentiometers precisely recorded vertical displacements in the mid-span. Load and displacement data were simultaneously monitored using a computer-aided eight-channel data acquisition system, and load-displacement relationships were graphically generated digitally based on the obtained data.

3. Results and discussions

In this study, the damage mechanisms, load carrying capacities, stiffness, ductility levels and energy consumption capacities of the specimens in each comparison group (CFRP areal weight, F-U-S- wrapping types, targeted concrete strength range) were evaluated in detail.

3.1. Test results

The beam test results examined within the scope of the study are summarized in Table 6. The symbols in this table, respectively. δ_y (mm);

Fig. 4. Application steps of reinforced concrete beam strengthening using the CFRP method.

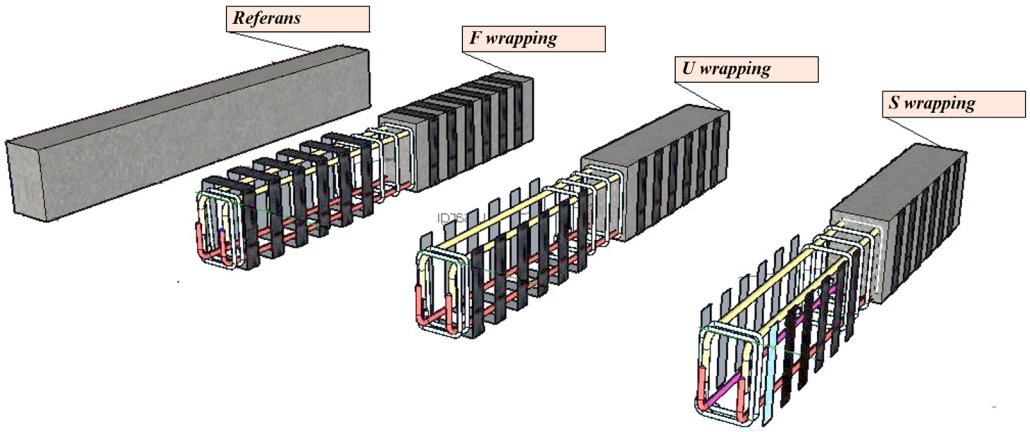

Fig. 5. Details of CFRP strengthening applied to the experimental beams.

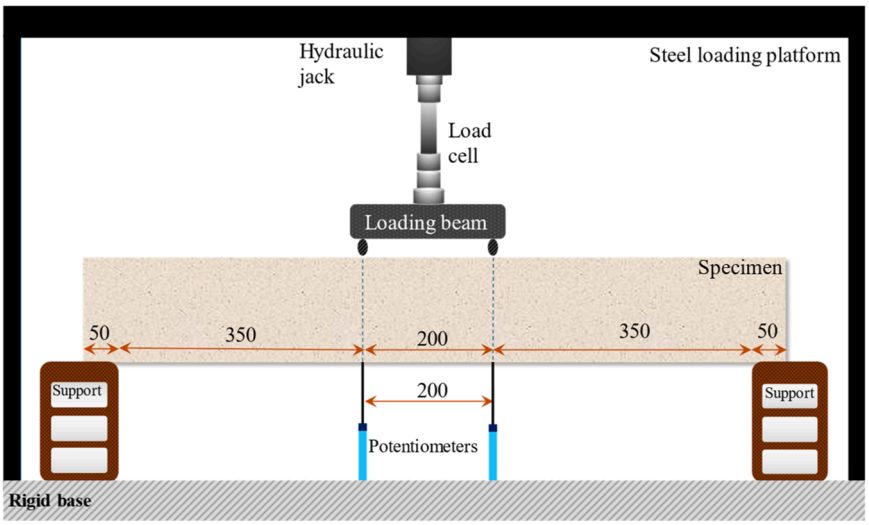

Fig. 6. Schematic representation of the experimental setup (Dimensions in mm).

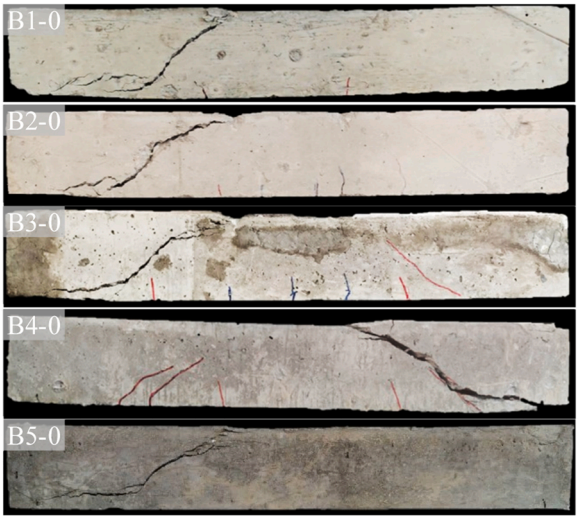

Fig. 7. Failure modes of the reference beam specimens at the end of the tests.

the displacement value at the $0.85P_{max}$ load level accepted as the yield point. δ_{max} (mm); the displacement value at the maximum load level. δ_u (mm); the displacement value at the $0.85P_{max}$ load level accepted as the rupture point. u; the ductility ratio. S_y (kN/mm); the stiffness at the yield point. S_{max} (kN/mm); the stiffness at the maximum load level. P_y (kN); the $0.85P_{max}$ load value accepted as the yield point. P_{max} (kN) represents the maximum load value. E_{yield} represents the energy consumption (kJ) up to the yield point, and E_{total} represents the total energy consumption (kJ). As a result of the experimental studies, the end-of-test failure mechanisms of the reference beam specimens are presented in Fig. 7, and the end-of-test failure mechanisms of the CFRP-strengthened beam specimens are presented in Fig. 8. The percentage increases in the load-carrying capacity of the strengthened beams compared to the reference specimens are presented in Fig. 9, while the increases in energy dissipation capacity in multiples are presented in Fig. 10. In addition, the ductility coefficients of the CFRP-strengthened beams are shown in Fig. 11.

3.2. Effect of concrete strength on strengthening performance

3.2.1. Load-carrying capacity

Experimental findings have shown that CFRP wrapping applications generally increase load-carrying capacity, but may have limited or negative effects in some concrete classes. Fig. 12 presents graphs comparing the load-displacement curves of CFRP-strengthened beams with respect to concrete strength, Fig. 13 illustrates the average values for each concrete strength range, along with error bars representing the standard deviations. Compared to the reference beam specimen, the change in load-carrying capacity of the strengthened beams occurred in different ranges depending on the concrete strength. As seen in Fig. 9, the rate of change for specimens with a target concrete compressive strength in the 5–10 MPa range varied between 2.4 % and 154.3 %. while this rate was −15.6 % and 109.4 % for specimens with a target concrete compressive strength in the 10–20 MPa range. In this study, the change was observed at −38.8 %–36.9 % for specimens with a target concrete compressive strength in the 30–40 MPa range, and it reached −17.9 %–40.7 % for specimens with a target concrete strength in the 50–60 MPa range. In specimens between 60 and 70 MPa, which represent the highest concrete strength, the change in load-carrying capacity was limited to 29.7 % and 47.2 %. These differences are due to the interaction mechanisms between the concrete's mechanical properties and CFRP. In low-strength concretes (5–20 MPa), premature cracking and large lateral deformations occur under loading due to their low modulus of elasticity and weak tensile capacity. This increases the effectiveness of CFRP, limiting crack propagation and strengthening the confinement effect. Furthermore, low-strength concretes exhibiting a high level of microcrack accumulation under loading tend to crack prematurely, resulting in earlier and more significant reductions in their load-carrying capacity. CFRP, on the other hand, intervenes at the point where the concrete begins to crack, limiting crack propagation and providing additional load-carrying capacity. Thus, the effect of CFRP on capacity becomes more pronounced in low-strength concretes.

Indeed, the load-carrying capacity increase reached 154.3 % in specimens with a target strength of 5–10 MPa and 109.4 % in the 10–20 MPa range. These values demonstrate the significant contribution of CFRP application to low-strength concrete. In contrast, in groups of 30–40 MPa and above, due to high stiffness, lateral deformation capacity is limited, and sudden cracks occur before failure, causing brittle fractures. This prevents the full effect of CFRP's confinement effect. Therefore, CFRP achieved a maximum capacity increase of 47.2 % in these groups.

Although capacity decreases were observed in some specimens in the medium-strength concrete group, this was attributed to application-related factors (such as inadequate epoxy impregnation, interface adhesion problems, or local application errors) rather than the theoretical contribution of CFRP. Overall, experimental findings indicate

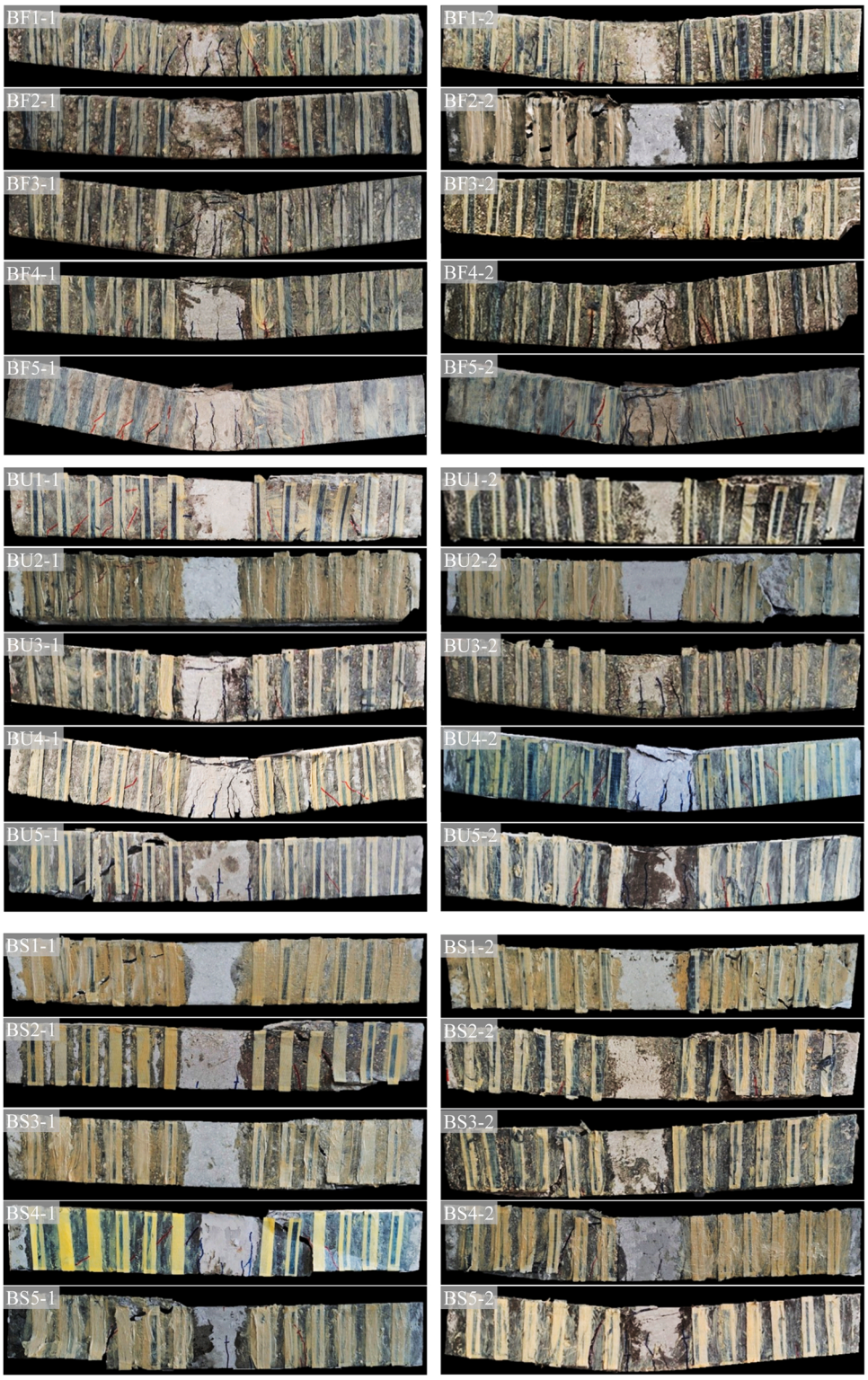

Fig. 8. Failure modes of the CFRP-strengthened beam specimens at the end of the tests.

that CFRP confinement significantly increases load-carrying capacity, particularly in low- and medium-strength concrete. Although the contribution of CFRP decreased as the concrete strength increased, the general trend compared to the reference was positive in all groups; the type and amount of wrapping also played a critical role in the carrying capacity by directly affecting these increase rates.

In addition to the general capacity trends, the nonlinear variations observed among concrete strength groups can be attributed to the complex interaction between the CFRP confinement mechanism and the evolving shear modulus of concrete during loading. As highlighted by Kalfas et al. [80], the effective stiffness of fiber-reinforced systems under coupled shear and flexural actions governs the redistribution of internal stresses, leading to nonlinear strength gains that vary with both confinement level and matrix deformability. This behavior was also reflected in the distinct load–displacement responses shown in Fig. 12, where low-strength concretes exhibited a gradual stiffness degradation,

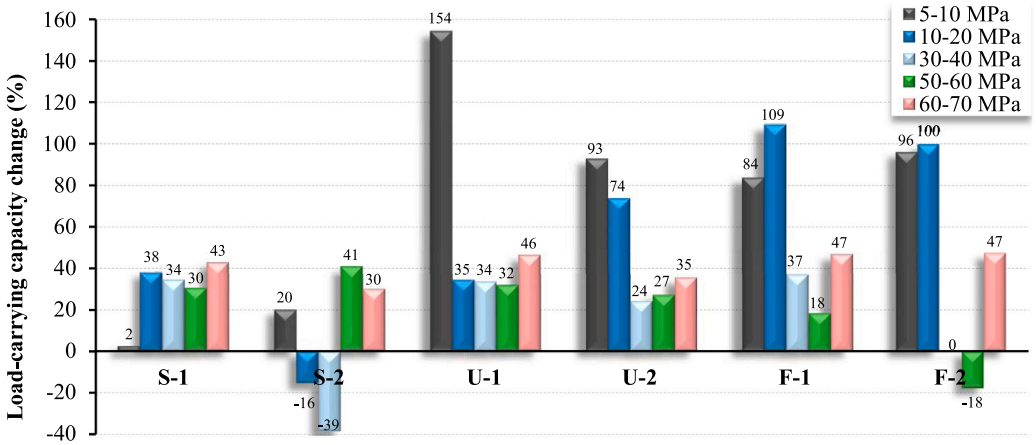

Fig. 9. Percentage increases in the load-carrying capacity of the strengthened beams compared to the reference specimens.

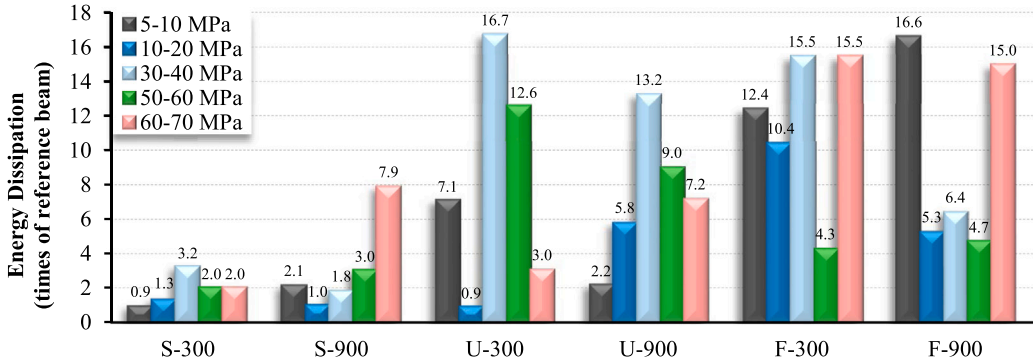

Fig. 10. Percentage increases in the energy dissipation capacities of the strengthened beams compared to the reference specimens. expressed in multiples.

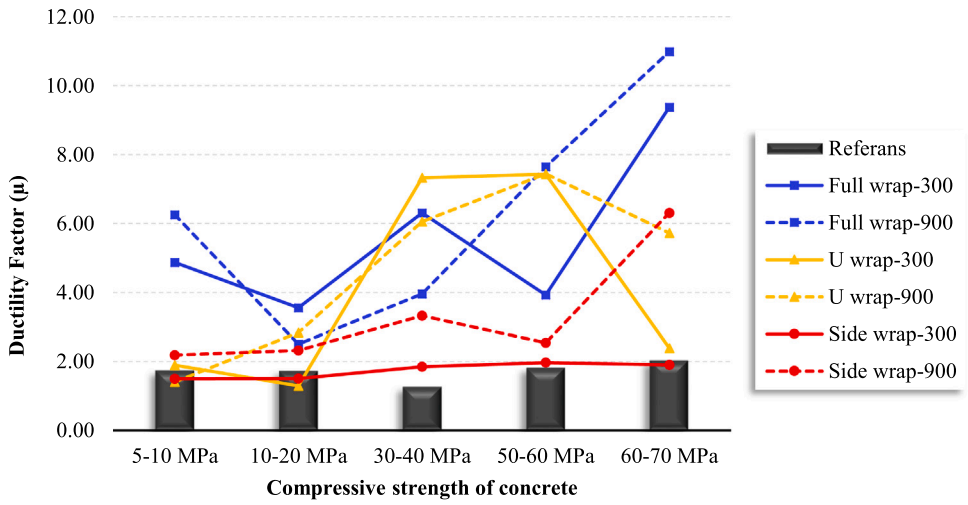

Fig. 11. Ductility coefficients of the CFRP-strengthened beams.

while higher-strength concretes demonstrated a brittle response dominated by localized bond stresses. Moreover, the stress redistribution patterns observed herein parallel the connector behavior in composite systems at elevated temperatures, as discussed in Davoodnabi et al. [81], reinforcing the consistency between experimental and numerical interpretations of CFRP bond performance under combined shear and thermal effects.

3.2.2. *Failure mode*

The failure mode was observed as shear failure in all reference specimens, and it was determined that the fracture behavior became more brittle as the concrete strength increased (Fig. 8). This indicates that, due to the more brittle structure of high-strength concretes, a sudden loss of capacity occurs after crack formation. After strengthening with CFRP, the failure mode changed in relation to concrete strength, and flexural failure was observed in some specimens.

In beams with very low-strength concretes (especially in the

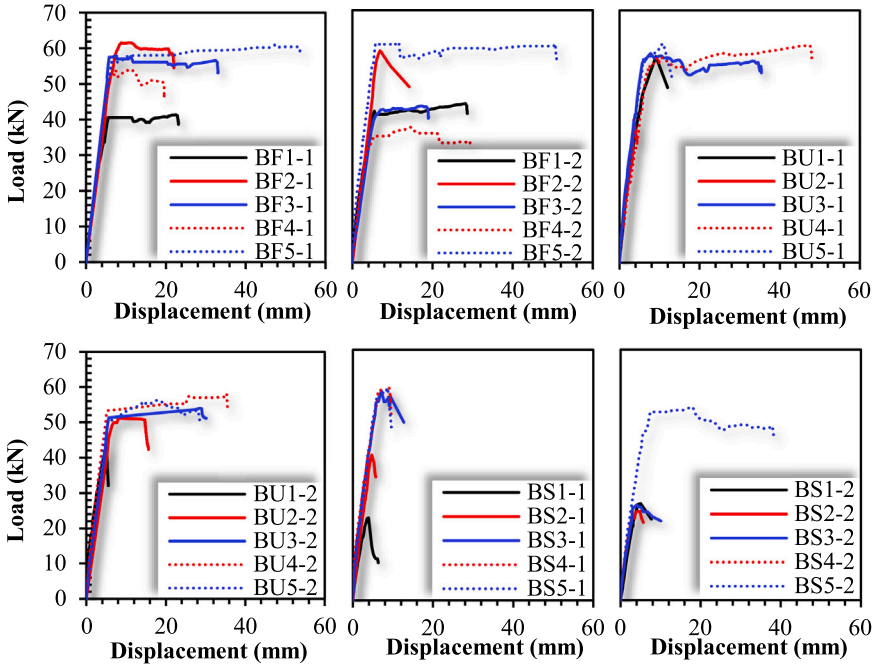

Fig. 12. Comparison of load–displacement curves according to concrete strength.

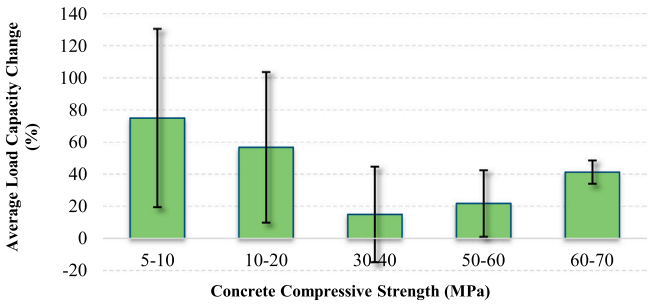

Fig. 13. Average load capacity increase for different concrete strength ranges with error bars representing standard deviations.

5–10 MPa and 10–20 MPa range), CFRP strengthening reveals a different failure mechanism compared to other concrete classes (Fig. 9). These types of concretes, due to their porous structure, low bond capacity, and weak compressive strength, have not fully utilized the potential of CFRP. Reliable increase in load-carrying capacity in strengthened elements depends on maintaining the bond between the CFRP layer and the concrete surface. However, because low-strength concrete has poor surface cohesion, the risk of adhesion loss and premature debonding at the epoxy-concrete interface is quite high. This prevents CFRP from operating at its full capacity, limits its strengthening effectiveness, and makes collapse more brittle. Therefore, regulations (e.g. ACI 440.2R-17 [73]) recommend a minimum concrete compressive strength of approximately 17 MPa for FRP applications other than full confinement. For lower-strength concrete, surface repair, the use of high-strength repair mortar, or alternative strengthening methods are recommended along with full confinement FRP applications. This has also been confirmed in experimental investigations; for example, peeling and rupture of the concrete cover were observed in beams with low concrete strengths, BU1–1, BU1–2, BU2–1 and BU2–2.

On the other hand, CFRP strengthening in reinforced concrete beams with compressive strengths in the 30–70 MPa range contributes significantly to both load-carrying capacity and collapse behavior. Adequate concrete compressive strength (minimum 25 MPa according to TBEC-2018) ensures reliable adhesion and load transfer of the CFRP layer, enabling CFRP to function effectively. After strengthening, the flexural capacity of beams in this strength class increases significantly, while the crack distribution becomes more uniform and the crack widths are more limited. As a result, the beam can carry higher loads until failure, and its deformation capability increases. Under bending, in particular, the contribution of CFRP in the tension zone increases ductility by compensating for the brittle behavior of the concrete. Thus, the beam exhibits a more controlled damage process rather than sudden, unprovoked failure. The damage mechanism most often occurs in the concrete compression zone as a result of buckling or partial CFRP debonding, but an energy consumption similar to plastic hinge formation is achieved before failure. Experiments have shown that approximately 61 % of beams with a concrete strength of 30 MPa and above converted the shear behavior observed in the reference beam specimen into flexural failure. Beyond the observed failure mechanisms, it is noteworthy that CFRP-strengthened beams also contribute to improved post-event performance and recovery potential. As discussed in Forcellini's study [1], similar strengthening systems have been shown to enhance performance continuity in bridge and building infrastructures, allowing for controlled damage progression and facilitating recovery after extreme events. This perspective reinforces the practical implications of CFRP confinement, demonstrating that its effectiveness extends not only to immediate load-carrying capacity and ductility but also to resilience-based design and maintenance considerations in structural applications.

3.2.3. *Energy dissipation, stiffness, and ductility*

As the concrete compressive strength in the test beams increases, the deformation capacity decreases due to the denser microstructure and less porous structure of the concrete. Accordingly, although all reference beams failed due to brittle fracture, low- and medium-strength concretes (5–40 MPa) exhibited relatively more ductile behavior, while high-strength concretes (50–70 MPa) exhibited much more brittle behavior. Energy dissipation up to yield point in the reference specimens remained in the range of 0.03–0.09 kJ and was quite limited. Similarly, ductility values ranging from 1.27 to 2.03 indicate that the beams failed due to brittle fracture, far from ductile behavior. The total energy dissipation capacity in the reference beam specimens was found to be in the range of 0.07–0.20 kJ. The observation of a tendency for rapid failure after cracking in unreinforced beams is consistent with these findings. As a

result of the strengthening applications carried out with CFRP composite, improvements were observed at different levels in the ductility properties and energy dissipation capacities of the beams depending on the concrete strength (Figs. 10 and 11). When evaluated in terms of total energy consumption, compared to the reference specimens, the change was 0.9–16.6 times in low-strength concretes in the 5–10 MPa range, and 0.9–10.4 times in specimens in the 10–20 MPa range. In the 30–40 MPa range, which represents the medium-strength concrete group, the changes reached 1.8–16.7 times, the highest values were obtained. On the other hand, the change varied between 2.0 and 12.6 times in specimens in the 50–60 MPa range, and was realized at 2.0–15.5 times in the 60–70 MPa range. The high proportional changess observed in beams, particularly in the 30–40 MPa range, are thought to be related to the fact that this strength group possesses sufficient compressive strength to effectively utilize the CFRP additive, that strong adhesion is achieved at the CFRP-concrete interface, and that debonding damage is avoided. Conversely, the more limited changes obtained in high-strength concretes and some low-strength specimens are largely due to CFRP-concrete bond performance and failure modes (e.g. debonding or concrete cover separation). Debonding has also been reported in the literature as a critical factor limiting CFRP effectiveness [82,83]. Additionally, the mechanisms observed here can be related to composite system behavior under extreme conditions, as discussed in Shariati et al. [84]. These studies support the view that CFRP confinement facilitates energy dissipation and ductile failure, linking the experimental findings to resilience-based design principles and demonstrating the robustness of CFRP-strengthened systems under both seismic and extreme loading scenarios. Strengthening applications with CFRP composites have also been found to have significant effects on the ductility coefficients of beams. According to the experimental results, the ductility coefficients were determined as 1.41–6.26 for the samples in the 5–10 MPa range, 1.29–3.56 for the 10–20 MPa range, 1.85–7.33 for the 30–40 MPa range, 1.97–7.65 for the 50–60 MPa range, and 1.90–10.99 for the 60–70 MPa range. The large difference between the lower and upper limits of the obtained values is due to the diversity in failure modes and the types of CFRP application. When the means are evaluated, the average ductility coefficients obtained in the low-strength concrete groups (5–10 and 10–20 MPa) are 3.02 and 2.34. respectively. which are below the value of approximately 4 recommended in the literature [85]. This shows that the strengthening applications with CFRP in these groups are limited in increasing ductility. In other words, it can be said that the effectiveness of CFRP in providing adequate ductility in the beam is limited. In contrast, the ductility coefficients for medium- and high-strength concrete in the 30–40. 50–60. and 60–70 MPa ranges were determined as 4.80, 5.16 and 6.11 respectively, meeting the minimum ductility criteria recommended in the literature for beams with sub-equilibrium designs.

Compared to the reference beam specimens, the pre-yield stiffness changes of the strengthened beams ranged from −5.51–36.56 % in the 5–10 MPa range, from −2.75–21.00 % in the 10–20 MPa range, from −31.65 to −4.63 % in the 30–40 MPa range, from −29.44 to −5.78 % in the 50–60 MPa range, and from −18.15–5.25 % in the 60–70 MPa range. The results indicate that CFRP strengthening can increase pre-yield stiffness to a certain extent in low-strength concretes (5–10 and 15–20 MPa). whereas it generally causes a decrease in stiffness in medium- and high-strength concretes (30–40. 50–60 and 60–70 MPa). This suggests that in low-strength concretes, CFRP contributes to elastic stiffness by delaying crack formation; however, in higher-strength concretes, cracks are transferred to the CFRP at an early stage, leading to a relative decrease in system stiffness. Furthermore, it can be argued that the reduction in stiffness provides greater deformation capacity until failure, thus paving the way for increased ductility. Therefore, this relative decrease in stiffness is not a negative consequence in terms of structural performance; on the contrary, it contributes to a safer fracture behavior by increasing energy absorption capacity and ductility.

3.3. Effect of CFRP fabric areal weight on strengthening performance

3.3.1. Load-carrying capacity

According to the results obtained from the specimens, when the effects of two different weights of CFRP applied to the beams were compared, no linear increase was observed with increasing weight. The comparative results between the two weights are presented in Fig. 14 via the load-displacement curves, Fig. 15 illustrates the average values for different CFRP fabric areal weights, along with error bars representing the standard deviations. Based on the experimental results, the contribution of the 900 g/m^2 CFRP wrapping to the load-carrying capacity compared to the 300 g/m^2 wrapping varied between 17.8 % and −73.2 % in the S series, 39.4 % and −61.4 % in the U series, and 12.4 % and −37.1 % in the F series. Although the CFRP strengthening applications provided an increase in load-carrying capacity of up to 154.3 % compared to the reference beams, when evaluated in terms of weight change, it is clearly seen that the increase has a limited effect on the load-carrying capacity. In fact, in some specimens (approximately 73 % of the beams), the 300 g/m^2 CFRP wrap achieved higher load-carrying capacity than the 900 g/m^2 wrap. Furthermore, it was observed that in no specimen (except BU5–1) the failure mechanism was caused by CFRP fabric failure; instead, it was limited to adhesion problems at the concrete-CFRP interface or concrete cover separation. These results demonstrate that 300 g/m^2 is sufficient for effective strengthening in the CFRP strengthening of the beams in this test group, while higher weight applications do not always provide additional benefits. It is believed that, particularly in CFRP applications with fabric thicknesses as high as 900 g/m^2, increasing fabric thickness triggers adhesion problems at the beam edge areas and creates application difficulties. Therefore, capacity increases were achieved at levels lower than 300 g/m^2 in some specimens. Therefore, 300 g/m^2 CFRP application offers the optimum solution in terms of both performance and ease of application, while choosing higher weights does not provide additional benefits in most cases and also increases costs and application risks.

3.3.2. Failure mode

Experimental findings indicate that CFRP weight has a limited effect on the damage modes developing in beams (Fig. 8). Only in specimens BU3–2, BU5–2, and BS5–2 did the failure mode change from shear to flexural failure when the CFRP fabric was increased from 300 g/m^2 to 900 g/m^2. No significant difference in the failure mode was observed in the other specimens. Furthermore, in none of the specimens did the failure mechanism occur directly through CFRP fabric failure (except BU5–1); damage was mostly limited to adhesion losses at the concrete-CFRP interface, occasional concrete cover separation, or partial debonding. Particularly in low-strength concretes (5–10 MPa), the dominant damage mechanism in 300 g/m^2 CFRP applications was shear failure due to concrete cover separation, while in 900 g/m^2 applications, the interface debonding effect became more pronounced due to increased thickness. Among the beams that failed by shear failure, no damage due to the concrete-CFRP interface was observed only in specimen BS1–2, while bond-related damage such as debonding and concrete cover separation was evident in all other specimens. These findings suggest that increasing CFRP thickness does not fundamentally alter the damage modes, but rather alters the predominance of the damage type in the existing weak zones. Similarly, the literature has reported that increasing CFRP layer thickness results in insufficient epoxy absorption, increasing the risk of debonding, particularly in the edge areas [86]. Therefore, the selection of the optimum weight for CFRP reinforcement is critical not only for its contribution to load capacity but also for controlling potential failure mechanisms. The use of higher weight (900 g/m^2) CFRP fabrics did not provide a significant improvement in beam behavior despite bringing additional costs. On the contrary, it had a negative effect on the interaction at the concrete-CFRP interface and had the potential to trigger undesirable damage types such as debonding and voids, bubbles or delamination in the epoxy layer.

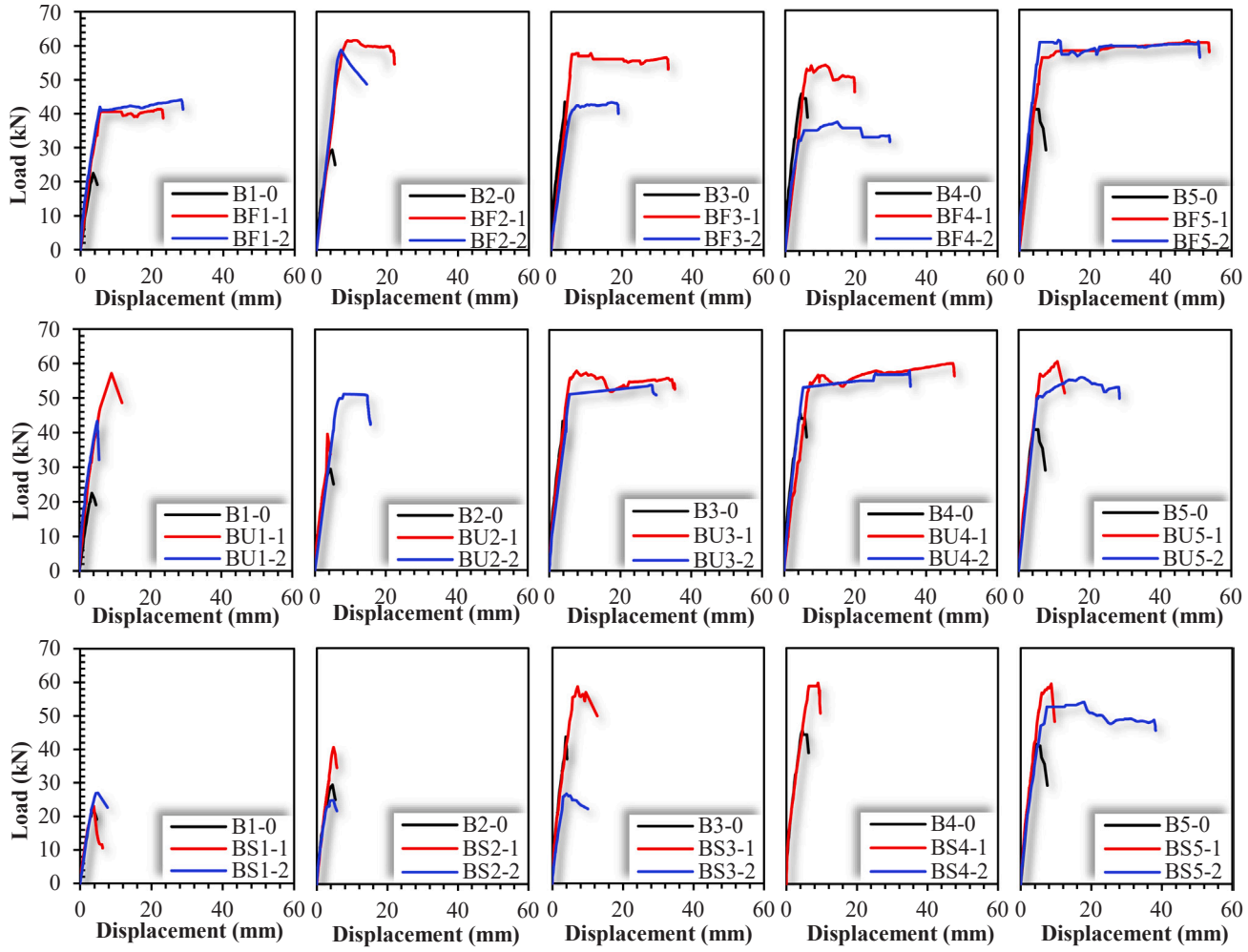

Fig. 14. Comparison of load–displacement curves according to CFRP areal weight.

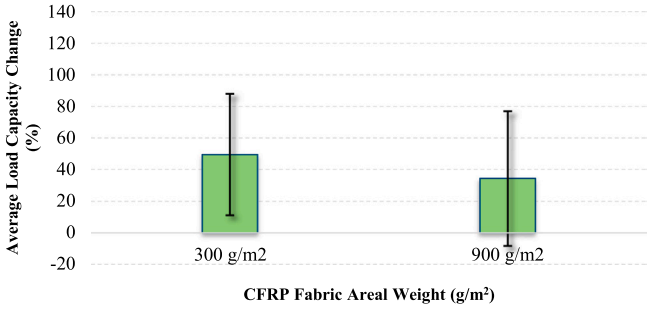

Fig. 15. Average load capacity increase for different CFRP fabric areal weights with error bars representing standard deviations.

3.3.3. *Energy dissipation, stiffness, and ductility*

When energy consumption was examined by weight, total energy consumption for beams with 300 g/m^2 application ranged from 1.0 to 16.61 times, while for beams with 900 g/m^2 application, the range was found to be 0.9–16.72 times. Furthermore, when switching from 300 g/m^2 to 900 g/m^2 for beams with the same physical properties, an increase in energy consumption was observed for only 46.7 % of beams, while a decrease occurred for the remaining 53.3 %. A similar distribution was observed for ductility coefficients. Based on these findings, it can be concluded that CFRP weight alone is not a decisive factor in improving energy consumption. Instead, higher weight applications can increase stress concentrations at the concrete-CFRP interface and problems with CFRP fibers not reaching full resin saturation, increasing the risk of premature debonding or cover separation. These mechanisms, in turn, can limit and sometimes reduce energy consumption. In practice, thinner and more saturated applications, such as 300 g/m^2, exhibit more stable and higher energy absorption behavior in most cases, while 900 g/m^2 applications are considered to provide additional benefits only when adhesion and application conditions (surface preparation. resin dosage. anchorage) are well controlled.

When examining the differences in stiffness at yield between 900 g/m^2 and 300 g/m^2 CFRP applications, it was observed that the results did not exhibit a consistent increasing trend. According to the obtained data, while the 900 g/m^2 CFRP application increased stiffness in approximately 40 % of the specimens, 60 % had lower stiffness values compared to the 300 g/m^2 application. This suggests that the effect of increasing CFRP weight on stiffness is not directly proportional and varies depending on the application conditions. In particular, increases reached up to + 2.40 in specimens with positive contributions, but losses of up to −2.61 were also observed in some specimens. Looking at the average values, it is noteworthy that the general trend is towards a loss of stiffness. The main reasons for this are the limited effectiveness of epoxy impregnation in high-weight CFRP sheets, incomplete filling of interfiber voids, and the formation of localized weaknesses at the interface. Therefore, the selection of CFRP weight should be optimized not only based on the target maximum capacity but also considering energy consumption/ductility/stiffness requirements and interface performance.

3.4. Effect of wrapping configuration on strengthening performance

3.4.1. Load-carrying capacity

Experimental results revealed significant differences in the load-carrying capacities of CFRP-strengthened beams depending on the type of wrapping. Fig. 16 presents a comparison of the load-displacement curves of CFRP-strengthened beams according to wrapping types. Fig. 17 illustrates the average values for different CFRP wrapping types, along with error bars representing the standard deviations. In specimens strengthened with F-type wrapping, the capacity change ranged from −18–109 %. with a significant increase compared to the reference beam in the majority of specimens. In this configuration, wrapping the entire circumference of the beam with CFRP provided an effective contribution in both compression and tension. With the exception of specimen BF2–2 in fully wrapped beams, CFRP was activated after the maximum load level was reached, allowing the post-load displacement capacity to be maintained, and the beams exhibited a significant bending behavior.

In specimens strengthened with U-type wrapping, the capacity increase ranged from −24–154 %. with some specimens achieving greater contributions compared to fully wrapped. This type of wrapping offers ease of application because it does not require intervention on the upper part of the concrete. It also significantly contributed to the shear and flexural capacity of the beam by encapsulating the side and bottom areas of the beam. The CFRP layers positioned on the side surfaces limited the propagation of shear cracks, improving load transfer stability, while the CFRP on the bottom surface supported flexural behavior in the tension zone. Furthermore, although a significant increase in load-carrying capacity was achieved in the BU1–1. BU1–2, and BU2–1 specimens with low-strength concrete, its contribution to displacement after the maximum load level was limited.

In specimens strengthened with the S-type, capacity changes ranged from −39–43 %. a very limited contribution compared to other wrapping types. Due to the limited surface load transfer in this configuration and the early onset of debonding damage, its contribution to the load-carrying capacity was minimal and contributed almost nothing to the displacement capacity. Therefore, it is considered more appropriate to consider side wrapping as a complementary or secondary strengthening technique rather than a standalone method.

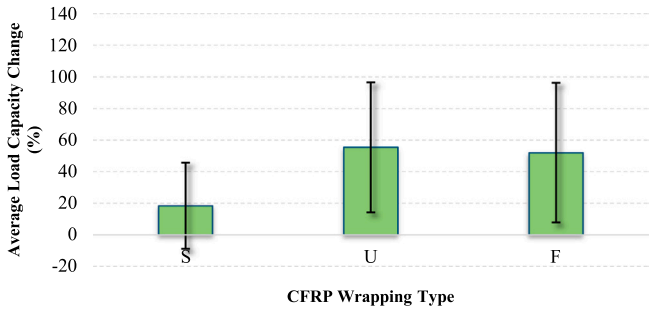

Fig. 17. Average load capacity increase for different CFRP wrapping types with error bars representing standard deviations.

3.4.2. Failure mode

The behavior of the reference beams that failed by shear failure changed significantly after CFRP strengthening (Fig. 9). Shear failure transitioned to flexural failure in approximately 90 % of the specimens with F-type wrapping, 40 % with U-type wrapping, and only 10 % with S-type wrapping. This demonstrates that the CFRP wrapping not only increases load-carrying capacity but also improves the structure's ductility by influencing the failure mode. This observation aligns with findings from Shariati et al. [87], which provides complementary insights into hybrid composite behavior and supports the understanding of combined CFRP–concrete interaction mechanisms in enhancing ductility and altering failure modes.

The F-type wrapping, created by enclosing the beam cross-section from four directions, significantly limited the propagation of shear cracks and virtually eliminated the risk of shear failure. Thus, the beams failed by flexural failure, a more ductile and predictive failure mode. Shear failure was observed only in specimen BF2–2. However, as seen in Fig. 8, it is noteworthy that the failure of this beam specimen occurred due to the incomplete absorption of the epoxy material and the formation of epoxy layering as a result of the use of 900 g/m^2 CFRP fabric.

The 40 % change in failure behavior in U-wrapped beams demonstrates that the method provides some effectiveness in controlling shear cracks, but is more limited than full-wrapped (F-type) beams. This difference stems from the CFRP's inability to fully support shear forces due

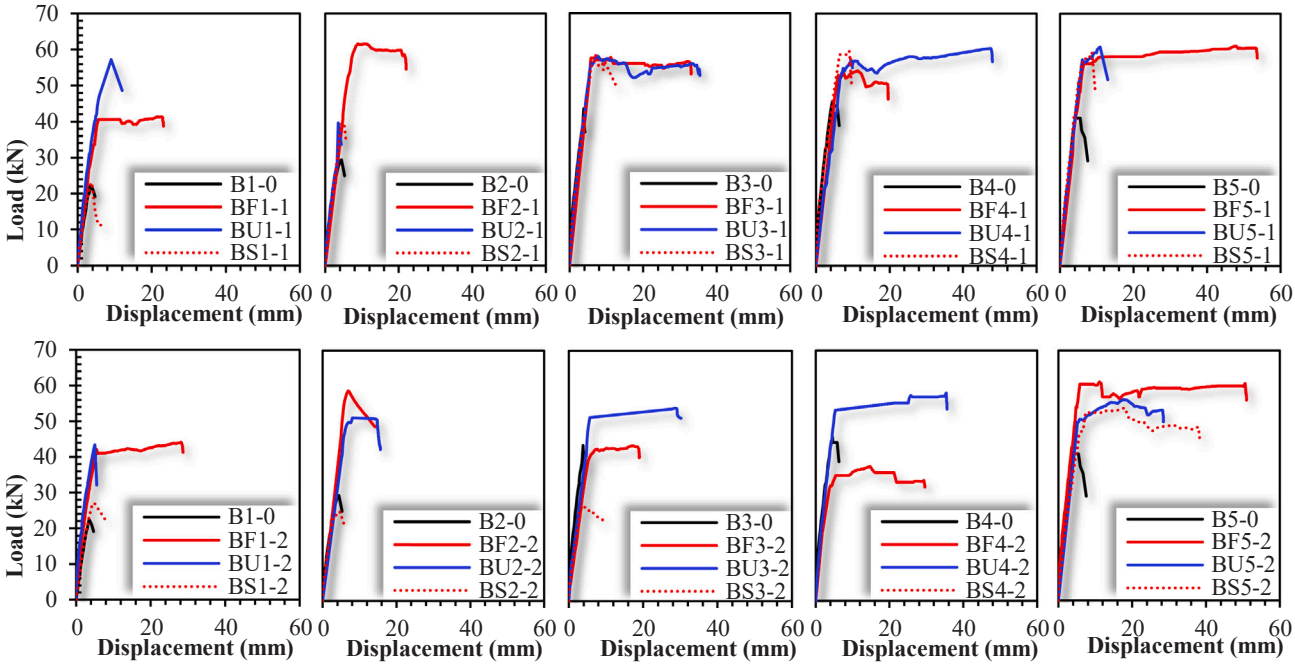

Fig. 16. Comparison of load-displacement curves according to CFRP wrapping type.

to the U-wrapped fiber ends remaining free and not being supported by additional anchors at the ends. Furthermore, defects such as debonding and separation of the CFRP-concrete cover observed in this group of beams also contributed to the failure of this strengthening. However, significant improvements were achieved in some specimens, indicating that additional anchoring details and application quality can enhance the effectiveness of U-type wrapping beams. Indeed, Aksoylu [26] also demonstrates that the use of horizontal wrappings to support U-type wrapping plays a critical role in enhancing the effectiveness of the strengthening. The S-type wrapping resulted in only a 10 % change in the failure mode. This can be explained by the fact that the side wrapping is effective only on the edge surfaces, the load transfer area is limited, and early debonding effects play a dominant role. Therefore, it was concluded that the side wrapping is insufficient to convert shear failure to flexural failure and should be considered more as a supplementary strengthening method.

3.4.3. Energy dissipation. stiffness. and ductility

When total energy consumption was examined by wrapping type, the energy consumption in beams with full wrapping (F) compared to the reference beam specimen varied between 4.26 and 16.61 times; in beams with U- wrapping (U), this value was found to be 0.90–16.72 times; and in beams with side wrapping (S), it was found to be 0.91–7.88 times. When the average values were taken into account, an increase of 10.60 times was observed for the F type, 7.77 times for the U type, and 2.54 times for the S type. These results clearly demonstrate that the type of CFRP application has a decisive effect on energy consumption.

The highest average energy consumption values in beams with full wrapping indicate that this method not only increases load-carrying capacity but also allows the beam to withstand greater deformation during the collapse process, thus imparting high ductility to the beams. Thus, full wrapping stands out as the most reliable method that simultaneously increases capacity and improves ductility. Total energy consumption in U-wrapped beams reached up to 16.72 times. This demonstrates that the method can be nearly as effective as full wrapping in some specimens. However, for beams other than specimens BU3–1. BU4–1. BU3–2, and BU4–2, the increase in energy consumption was largely due to the increase in load capacity, while deformation capacity remained limited. In other words, although the load-carrying capacity of approximately 60 % of the beams strengthened with U-wrapped beams significantly exceeded that of the reference beams, the increase in ductility was limited. This suggests that application details such as inadequate anchorage or exposed fiber ends can lead to a decrease in energy consumption.

For beams with side wrapping, energy consumption was limited to an average increase of 2.54 times, This increase was largely due to a partial improvement in load-carrying capacity, with only the BS5–2 specimen achieving a high value (ductility coefficient = 6.31) due to deformation capacity. However, the fact that ductility values in beams other than this specimen remained below 3.32 suggests that the contribution of the side wrapping to energy consumption is generally low.

It is also noteworthy that energy consumption and ductility coefficients are consistent. Ductility coefficients were found to range from 2.50 to 10.99 in beams with F-type windings, 1.29–7.43 in U-type windings, and 1.50–6.31 in S-type windings. The particularly high value (6.31) in the BS5–2 sample is an exception and deviates from the general trend. The stiffness values at yield point were determined to range from 7.40 to 10.34 in F-type wrapping, 7.67–10.72 in U-type wrapping, and 6.72–10.72 in S-type wrapping. These results indicate that wrapping type has a limited effect on stiffness up to yield point.

3.5. Code-based analytical evaluation

The experimental study investigated the shear behavior of reinforced concrete beams strengthened with CFRP fabrics of different configurations, varying in both fiber weight and wrapping type. The results obtained from the experiments were compared with analytical calculations based on various design codes, including TBEC-2018, ACI 440.2R-17 and FIB-2010. To examine the influence of wrapping configuration and fiber weight on the shear performance of the beams, Table 9 and Fig. 18 were prepared. In the experimental program, three different wrapping types-full wrapping (F), U-wrap (U), and side-face wrapping (S)-were applied. Moreover, two types of CFRP fabrics with different fiber weights, 300 g/m^2 and 900 g/m^2, were utilized. The analytical study was conducted using these experimental data to evaluate how the selected parameters affect the shear strength and to compare the findings with code-based predictions. The prediction models and the design equations used in this study are summarized in Table 8.

The shear capacity of a standard reinforced concrete beam is calculated by considering the contributions of transverse reinforcement (V_s) and concrete (V_c). However, when the beam is wrapped with FRP, the contribution of the fiber (V_f) is also added to the shear capacity.

Within the scope of TBEC-2018, the total shear capacity of the beam was calculated using the summation relationship given in Equation (3). The V_c value, which represents the contribution of concrete to shear capacity, was taken as 80 % of the value obtained from Equation (1), Equation (2) expresses the contribution of CFRP wraps to the shear effect. In TBEC-2018, only full wrapping (F-type) strengthening is considered; therefore, F-type strengthening was taken as the basis for Table 8. In addition, Table 5 presents the mechanical properties of the CFRP material used for strengthening in the experimental study, and these properties were also considered as input parameters in the analytical formulations.

In the ACI 440.2R-17 code, the strengthening of beams is determined similarly to TBEC-2018, by the sum of the contributions of concrete, stirrups, and FRP wraps to shear capacity. The contribution of the wrap to shear capacity was calculated using Equation (4), and the FRP area and strength values in this equation were obtained with the help of Equations (5) and (6). When calculating the effect of the wrap in ACI 440.2R-17, the spacing values depending on the continuity of the wrap are determined using Equation (8). However, in this study, CFRP strips were applied discontinuously (with gaps), and this continuity condition was not included in the calculations.

In the FIB-2010 code, the contribution of FRP to shear capacity is calculated using Equation (9). In these calculations, which consider the wrapping type and fiber weight details, the obtained values were compared with experimental results.

Calculations could only be performed for unstrengthened cases and F-wrapped specimens according to TBEC-2018. In the experimental study, specimen B1–0 exhibited 27 % higher load-bearing capacity, B2–0 8 %, and B3–0 4 % higher values. In specimens B4–0 and B5–0, the load-bearing capacities gave close values of 93 % and 76 %, respectively. In F-type wrapping with low fiber weight, average close results of 68 % were obtained for all concrete strengths, while a close value of 85 % in specimen BF2–1 is noteworthy. For concrete class C20 and below, the contribution of F-type wrapping to load-bearing capacity is much higher than for other strengths. In TBEC-2018, a threefold increase in CFRP fiber weight is expected to increase load-bearing capacities by 2.91 times, but the experimental results did not show the same rate of increase. Nevertheless, for both fiber weights, F-type wrapping gave very close values for shear capacity in many concrete strengths. Since TBEC-2018 does not provide calculations for U and S-type wrapping, the experimental results for these wrapping types could not be compared.

Without strengthening according to ACI 440.2R-17, the obtained results were significantly lower than the experimental results. In the experimental study, the load-bearing values were 70 % higher for B1–0, 44 % for B2–0, and 39 % for B3–0 compared to the analytical calculations. In specimens with concrete class C30 and above, this ratio decreased to 2 %. The experimental results obtained with F-type

Table 7
Test results for all beam specimens.

Specimen Number	δ_y (mm)	δ_{max} (mm)	δ_u (mm)	u (δ_u/δ_y)	S_y (kN/mm)	S_{max} (kN/mm)	P_{max} (kN)	P_u (kN)	E_{yield} (kJ)	E_{total} (kJ)	Mode of failure
B1–0	2.69	3.48	4.68	1.74	7.12	6.46	22.49	19.12	0.03	0.07	S
B2–0	3.04	4.42	5.25	1.73	8.23	6.66	29.42	25.01	0.05	0.11	S
B3–0	3.29	3.83	4.16	1.27	11.24	11.36	43.51	36.98	0.08	0.11	S
B4–0	3.46	4.53	6.29	1.82	11.25	10.10	45.74	38.87	0.09	0.20	S
B5–0	3.32	4.21	6.74	2.03	10.64	9.87	41.57	35.34	0.06	0.19	S
BF1–1	4.75	22.53	23.16	4.88	7.40	1.83	41.34	35.13	0.10	0.84	F
BF2–1	6.19	10.91	22.04	3.56	8.46	5.65	61.61	52.37	0.17	1.11	F
BF3–1	5.25	10.13	33.07	6.31	9.65	5.88	59.55	50.62	0.14	1.68	F
BF4–1	4.99	11.34	19.63	3.93	9.21	4.77	54.11	45.99	0.12	0.87	F
BF5–1	5.73	47.33	53.69	9.37	9.05	1.29	60.99	51.84	0.15	2.98	F
BF1–2	4.59	28.21	28.71	6.26	8.17	1.56	44.13	37.51	0.11	1.13	F
BF2–2	5.28	6.88	13.22	2.50	9.46	8.54	58.76	49.95	0.14	0.56	S
BF3–2	4.80	16.97	19.01	3.96	7.68	2.56	43.40	36.89	0.10	0.70	F
BF4–2	3.86	14.76	29.54	7.65	8.26	2.54	37.54	31.91	0.07	0.97	F
BF5–2	4.64	11.10	51.02	10.99	11.20	5.51	61.21	52.03	0.15	2.89	F
BU1–1	6.34	9.08	12.00	1.89	7.67	6.30	57.20	48.62	0.33	0.48	S
BU2–1	3.38	3.56	4.37	1.29	9.96	11.14	39.59	33.65	0.07	0.10	S
BU3–1	4.83	7.74	35.41	7.33	10.22	7.50	58.09	49.38	0.13	1.82	S
BU4–1	6.46	47.14	47.99	7.43	7.94	1.28	60.31	51.26	0.17	2.57	F
BU5–1	5.43	10.94	13.00	2.39	9.51	5.56	60.82	51.7	0.15	0.59	S
BU1–2	3.80	5.04	5.33	1.41	9.72	8.62	43.39	36.88	0.09	0.15	S
BU2–2	5.44	8.06	15.47	2.84	7.99	6.35	51.18	43.5	0.12	0.62	S
BU3–2	4.98	28.61	30.19	6.06	9.21	1.89	54.01	45.91	0.13	1.44	F
BU4–2	4.78	35.33	35.59	7.44	10.34	1.65	58.13	49.41	0.13	1.84	F
BU5–2	4.97	17.55	28.47	5.72	9.61	3.20	56.21	47.78	0.12	1.38	F
BS1–1	2.83	3.87	4.23	1.50	6.92	5.95	23.03	19.57	0.03	0.06	S
BS2–1	3.78	4.73	5.70	1.51	9.13	8.58	40.60	34.51	0.07	0.14	S
BS3–1	4.64	6.34	8.58	1.85	10.72	9.22	58.47	49.70	0.13	0.35	S
BS4–1	4.88	8.99	9.60	1.97	10.38	6.64	59.63	50.69	0.14	0.41	S
BS5–1	4.95	8.67	9.43	1.90	10.19	6.85	59.36	50.46	0.14	0.39	S
BS1–2	3.42	4.96	7.47	2.19	6.72	5.46	27.04	22.98	0.05	0.14	S
BS2–2	2.45	4.30	5.69	2.32	8.60	5.78	24.84	21.11	0.03	0.11	S
BS3–2	2.79	3.98	9.28	3.32	8.11	6.69	26.63	22.63	0.04	0.20	S
BS4–2	5.16	12.23	13.14	2.55	10.60	5.26	64.36	54.7	0.14	0.62	S
BS5–2	5.26	15.86	33.20	6.31	8.71	3.40	53.93	45.84	0.14	1.52	F

*In terms of failure mode. the symbol S represents shear failure. while F represents flexural failure.

Table 8
The prediction models and the design equations.

Design guide	General expression		Full wrapping		Continuous strips	
TBEC-2018	$V_{cr} = 0.65 \times f_{ctm} \times b_w \times d \times \sqrt{1 + \frac{N}{A_c \times f_{ctm}}}$	(1)	$V_r = V_c + V_w + V_f$	(3)		
	$V_f = \frac{2n_f t_f w_f E_f \varepsilon_f d}{s_f}$	(2)				
ACI 440.2R-17	$V_f = \frac{A_{fv} \times f_{fe} \times (\sin\alpha + \cos\alpha) \times d_{fv}}{s_f}$	(4)	$\varepsilon_{fe} = 0.004 \leq 0.75.\varepsilon_{fu}$	(7)		
	$A_{fv} = 2 \times n \times t_f \times w_f$	(5)			$s_f = w_f$	(8)
	$f_{fe} = \varepsilon_{fe} \times E_f$	(6)				
FIB-2010	$V_{fd} = 0.9 \times \varepsilon_{fd} \times E_{fu} \times \rho_f \times b_w \times d \times(\cot\theta + \cot\alpha) \times \sin\alpha$	(9)	$\varepsilon_{fd,e} = 0.17\left(\frac{f_c{}^{2/3}}{E_{fu}.\rho_f}\right)^{0.30} \times \varepsilon_{fu}$	(10)	$\rho_f = 2 \times t_f \times \frac{\sin\alpha}{b_w}\rho_f = 2 \times \left(\frac{t_f}{b_w}\right) \times \left(\frac{b_f}{s_f}\right)$	(11)

wrapping were much lower than the analytical calculations according to ACI 440.2R-17. In the experimental results obtained with low fiber weight, the maximum load-bearing capacities approached the predicted values of the code by 73 % for BF1–1, 97 % for BF2–1, 80 % for BF3–1, 68 % for BF4–1, and 73 % for BF5–1. However, the results for high fiber weight CFRP were predicted to be much higher in ACI 440.2R-17. Nevertheless, for all concrete strengths, the maximum load-bearing capacities remained limited to 23–40 % of analytical calculations. In the experimental results, the contributions of the two fiber weights were close, and especially in specimens with concrete class C30 and above, the contribution of low fiber weight was higher. From this, it was observed that the effect of the FRP fiber weight used in strengthening decreases once the concrete strength exceeds a certain level.

In FIB-2010, the predicted capacities without strengthening were lower than the experimental results. In the experimental results, the maximum load-bearing capacities were 70 % higher for B1–0, 44 % for B2–0, 39 % for B3–0, 24 % for B4–0, and 2 % for B5–0 compared to analytical calculations. When the contribution of low fiber weight CFRP in F-type wrapping was included, the expected increase in analytical calculations appeared as an average of 88 % for concrete strengths below C20 and approximately 63 % for higher strengths. Again, as the concrete strength increased, the effect of CFRP decreased. For high CFRP fiber weight, the experimental results reached only 48 % for BF1–2, 51 % for BF2–2, 30 % for BF3–2, 24 % for BF4–2, and 37 % for BF5–2 of the analytically predicted values. According to FIB-2010, predictions for maximum load-bearing capacity in U-type wrapping were much lower than the experimental results for low-strength concrete, showing that concrete strength, particularly for C20 and below, has a more effective impact. In concrete classes C20 and above, maximum load-bearing capacities with low fiber weight CFRP remained at an average of 52 % of

Table 9
Experimental and analytical maximum shear forces (kN).

Test Specimens	Shear Force (P/2)	ACI 440.2R-17			FIB-2010			TBEC-2018		
	V_r	V_f	V_c+V_s	V_r	V_f	V_c+V_s	V_r	V_f	V_c+V_s	V_r
B1–0	11.25	-	6.60	6.60	-	6.60	6.60	-	8.83	8.83
B2–0	14.71	-	10.21	10.21	-	10.21	10.21	-	13.67	13.67
B3–0	21.76	-	15.69	15.69	-	15.69	15.69	-	21.00	21.00
B4–0	22.87	-	18.39	18.39	-	18.39	18.39	-	24.61	24.61
B5–0	20.79	-	20.38	20.38	-	20.38	20.38	-	27.27	27.27
BF1–1	20.66	21.57	6.60	28.18	18.71	6.60	25.31	22.40	8.83	31.24
BF2–1	30.80	21.57	10.21	31.79	22.28	10.21	32.49	22.40	13.67	36.08
BF3–1	29.77	21.57	15.69	37.27	26.45	15.69	42.15	22.40	21.00	43.41
BF4–1	27.05	21.57	18.39	39.97	28.18	18.39	46.58	22.40	24.61	47.02
BF5–1	30.49	21.57	20.38	41.96	29.37	20.38	49.75	22.40	27.27	49.68
BF1–2	22.06	62.66	6.60	69.27	39.46	6.60	46.06	65.07	8.83	73.91
BF2–2	29.38	62.66	10.21	72.88	46.99	10.21	57.21	65.07	13.67	78.74
BF3–2	21.70	62.66	15.69	78.36	55.79	15.69	71.49	65.07	21.00	86.07
BF4–2	18.76	62.66	18.39	81.05	59.45	18.39	77.84	65.07	24.61	89.68
BF5–2	30.60	62.66	20.38	83.05	61.95	20.38	82.33	65.07	27.27	92.35
BU1–1	28.59	16.51	6.60	18.15	0.37	7.68	8.06	-	-	-
BU2–1	19.79	16.51	10.21	26.15	0.51	18.36	18.87	-	-	-
BU3–1	29.04	16.51	15.69	45.00	0.71	43.49	44.20	-	-	-
BU4–1	30.15	16.51	18.39	57.13	0.80	59.67	60.47	-	-	-
BU5–1	30.41	16.51	20.38	67.38	0.86	73.32	74.19	-	-	-
BU1–2	21.69	48.81	6.60	42.37	0.60	7.68	8.29	-	-	-
BU2–2	25.58	48.81	10.21	50.38	0.83	18.36	19.19	-	-	-
BU3–2	27.00	48.81	15.69	69.22	1.15	43.49	44.64	-	-	-
BU4–2	29.06	48.81	18.39	81.36	1.29	59.67	60.96	-	-	-
BU5–2	28.10	48.81	20.38	91.60	1.39	73.32	74.72	-	-	-
BS1–1	11.51	16.51	7.68	24.19	0.37	7.68	8.05	-	-	-
BS2–1	20.29	16.51	18.36	34.87	0.51	18.36	18.87	-	-	-
BS3–1	29.23	16.51	43.49	60.00	0.71	43.49	44.20	-	-	-
BS4–1	29.81	16.51	59.67	76.18	0.80	59.67	60.47	-	-	-
BS5–1	29.68	16.51	73.32	89.83	0.86	73.32	74.18	-	-	-
BS1–2	13.51	48.81	7.68	56.49	0.60	7.68	8.28	-	-	-
BS2–2	12.41	48.81	18.36	67.17	0.83	18.36	19.19	-	-	-
BS3–2	13.31	48.81	43.49	92.30	1.15	43.49	44.64	-	-	-
BS4–2	32.17	48.81	59.67	108.48	1.29	59.67	60.96	-	-	-
BS5–2	26.96	48.81	73.32	122.13	1.39	73.32	74.71	-	-	-

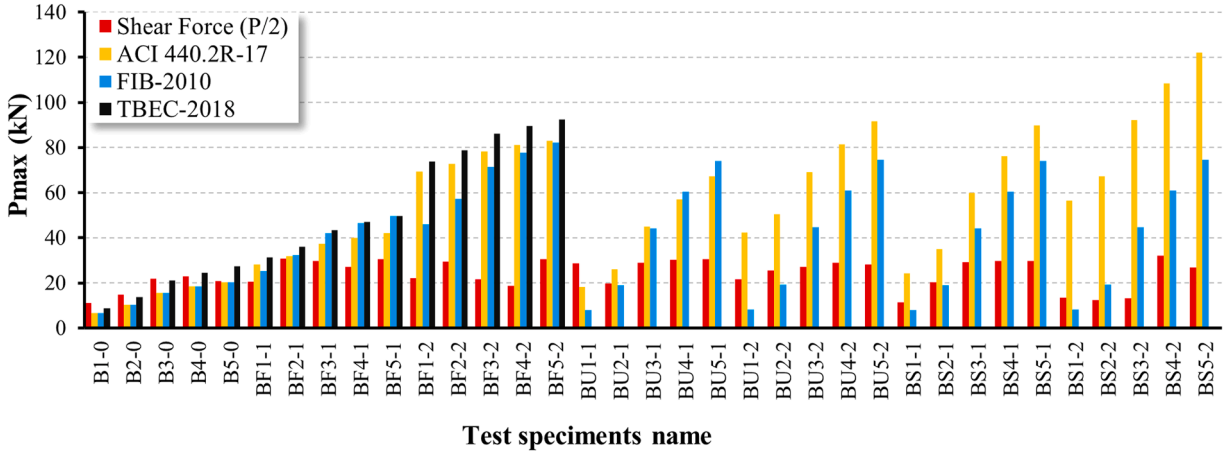

Fig. 18. Compare the test specimens and their P_{max} values.

analytical predictions, and similarly for high fiber weight at 49 %. The lower-than-expected increase with fiber weight indicates that the effect of fiber weight on beam shear capacity is limited. Additionally, increasing concrete strength above C20 significantly reduces the contribution of strengthening.

4. Conclusions

In this study. the effectiveness of CFRP strengthening on reinforced concrete beams with insufficient shear capacity was experimentally investigated, taking into account concrete strength, CFRP areal weight, and wrapping type. A total of 35 one-third scale beam specimens, representing different concrete strengths, three CFRP wrapping configurations, and two CFRP areal weights, were tested under four-point bending. The damage mechanisms, load-carrying capacities, stiffness, ductility, and energy dissipation capacities of the reference and strengthened beams were comparatively evaluated. The main findings can be summarized as follows:

1. The experimental results indicated that all CFRP wrapping applications increased the load-carrying capacity of beams across the full range of concrete strengths. In low-strength concretes (5–20 MPa), CFRP engaged earlier due to early cracking and large deformation tendencies, resulting in capacity enhancements of up to 154.3 %. In contrast, in relatively higher-strength beams (≥30 MPa), the contribution of CFRP was limited because of increased stiffness and brittle failure tendencies, with a maximum improvement of 47.2 %. These findings demonstrate that the effectiveness of CFRP is directly related to the mechanical properties of the concrete and that CFRP provides a particularly efficient strengthening strategy in terms of load-carrying capacity for low- to medium-strength concretes.
2. The failure mode of all reference beams was observed as shear failure, with increasing concrete strength resulting in more brittle fractures. Following CFRP strengthening, approximately 61 % of beams with concrete strengths between 30 and 70 MPa experienced a shift in failure mode from shear to flexure, with a more controlled crack distribution and enhanced deformation capacity. In contrast, for low-strength concretes (5–20 MPa), only 25 % of beams exhibited a change from shear to flexural failure; the effectiveness of CFRP in improving the failure mode was limited, and sudden, brittle failure occurred due to early debonding. These findings indicate that a minimum concrete compressive strength is critical for CFRP strengthening, and compliance with the approximate 17 MPa lower limit recommended by ACI 440.2R-17 [73] is necessary.
3. CFRP strengthening significantly enhanced both the energy dissipation capacity and ductility of the beams, depending on the concrete strength. The total energy dissipation increased by 0.9–16.6 times for low-strength concretes (5–20 MPa), 1.8–16.7 times for concretes in the 30–40 MPa range, and 2.0–15.5 times for high-strength concretes (50–70 MPa). while the ductility indices ranged from 1.29 to 6.26 1.85–7.33 and 1.90–10.99 respectively. It can be concluded that CFRP effectively improved both energy dissipation and ductility in concretes with strengths of 30–40 MPa, while also ensuring controlled deformation in higher-strength concretes.
4. The experiments demonstrated that the effect of CFRP areal weight on the load-carrying capacity of beams was not linear. The 900 g/m^2 wrapping provided contributions ranging from + 17.8 % to –73.2 % in the S series, + 39.4 % to –61.4 % in the U series, and + 12.4 % to –37.1 % in the F series, compared to 300 g/m^2. In fact, approximately 73 % of the beams exhibited greater load-carrying capacity improvements with the 300 g/m^2 wrapping than with the higher areal weight applications. Therefore, the 300 g/m^2 CFRP application offers an optimal solution in terms of both effectiveness and ease of application, while higher areal weights do not provide additional benefits and increase costs and application risks.
5. The CFRP areal weight was found to have a limited effect on the failure modes of the beams; a shift from shear to flexural failure occurred only in specimens BU3–2. BU5–2, and BS5–2, while no such change was observed in the others. In no specimen did the failure mechanism occur directly due to CFRP rupture (except BU5–1); damages were mostly confined to loss of bond at the concrete–CFRP interface, cover separation, or partial debonding. These findings indicate that, despite the additional cost of high areal weight CFRP, it does not provide a significant improvement in beam behavior and may increase the risk of debonding and epoxy layer delamination, highlighting that selecting an optimal areal weight is critical.
6. The total energy dissipation changed by 1.0–16.61 times for the 300 g/m^2 applications and by 0.9–16.72 times for the 900 g/m^2 applications; however, upon increasing to 900 g/m^2. energy gains were observed in only 46.7 % of the specimens, while 53.3 % experienced a decrease. The ductility indices exhibited a similar trend. No consistent trend was observed in terms of stiffness; 900 g/m^2 applications resulted in increases in only 40 % of the specimens, while 60 % showed a reduction, with the overall tendency being a loss of stiffness. These results suggest that, due to insufficient epoxy impregnation and interfacial weaknesses, the additional benefits of high areal weight CFRP are limited in most cases compared to 300 g/m^2 applications.
7. Among the wrapping configurations. the F- and U-type applications proved to be the most effective methods, providing load-carrying capacity increases of up to 154 %. In particular. F-type applications also enhanced the post-peak displacement capacity, thereby improving flexural behavior. In contrast, the side-only wrapping contributed less than 43 % and exhibited limited deformation capacity due to early debonding, making it insufficient as a standalone strengthening method. Consequently, side wrapping should be considered as a complementary rather than a primary technique.
8. The failure mode shifted from shear to flexure depending on the CFRP wrapping type, with conversion rates of 90 % for F-type wrapping, 40 % for U-type, and only 10 % for side wrapping. Full wrapping nearly eliminated shear failure, enabling ductile flexural failure, while U-type wrapping was limited due to anchorage deficiencies and debonding. Although side-only wrapping had a limited effect on changing the failure mode, it may play a role in controlling local cracking when used in combination with other methods.
9. The highest average increase in energy dissipation was achieved with F-type wrapping (10.60 times), followed by U-type wrapping at 7.77 times, while the contribution of side-only wrapping was quite limited (2.54 times). F-type wrapping proved to be the most effective method, simultaneously enhancing both capacity and ductility. Although U-type wrapping was effective in terms of capacity gain, its deformation capability was more limited. For side-only wrapping, ductility values mostly remained below the recommended minimum, providing insufficient contribution to energy dissipation.

This study systematically investigated the effects of CFRP strengthening on the shear behavior of reinforced concrete beams through comprehensive experimental tests considering different concrete strengths, CFRP areal weights, and wrapping configurations. The findings demonstrate that CFRP provides significant improvements in load-carrying capacity, ductility, and energy dissipation, particularly for beams with insufficient shear capacity. However, the performance is critically influenced by application details, including wrapping type, bond conditions, and areal weight selection. Notably, 300 g/m^2 CFRP applications were generally more effective than 900 g/m^2, indicating that optimal material usage is not only economically advantageous but also strategically important for structural reliability. Additionally, the use of only 2Ø10 reinforcement in the tensile zone and 30 mm-wide CFRP strips resulted in a shift of the failure mode from shear to flexure in both 300 g/m^2 and 900 g/m^2 applications, limiting the observable effect of areal weight differences. Therefore, it is anticipated that beams with higher flexural reinforcement and varied strip widths would more clearly reveal the performance benefits of 900 g/m^2 CFRP. The ability of CFRP to convert shear failures predominantly into ductile flexural failures confirms the method's potential to provide safe and controlled failure mechanisms. Future studies investigating long-term performance and seismic behavior of CFRP applications under different concrete grades, anchorage details, and environmental conditions are crucial for enhancing the reliability of the method in practical engineering applications and for informing the development of current design guidelines.

CRediT authorship contribution statement

ARSLAN Musa Hakan: Writing – review & editing, Writing – original draft, Validation, Supervision, Methodology, Conceptualization. **SARI ALAV Deniz:** Writing – original draft, Investigation, Data curation. **UYSAL Yusuf:** Writing – original draft, Visualization, Methodology, Investigation, Formal analysis, Data curation. **AKSOYLU Ceyhun:** Writing – review & editing, Writing – original draft, Supervision, Methodology, Investigation.

Declaration of Generative AI and AI-assisted technologies in the writing process

During the preparation of this work, the authors used ChatGPT in order to improve several important aspects of writing, such as readability, grammar, spelling, and tone of the text. After using this tool, the authors reviewed and edited the content as needed and take full responsibility for the content of the publication.

Declaration of Competing Interest

The authors declare that they have no known competing financial interests or personal relationships that could have appeared to influence the work reported in this paper.

Acknowledgments

This study was prepared by using the master thesis of Deniz SARI ALAV. The study was also supported by the Scientific Research Projects Unit of Konya Technical University under project number 211004041. The opinions expressed in this paper are those of the authors and do not reflect the views of the sponsor.

References

[1] Forcellini D. Quantification of the Seismic Resilience of Bridge Classes. J Infrastruct Syst 2024;30:04024016. https://doi.org/10.1061/JITSE4.ISENG-2376.
[2] Bagheri M, Ranjbar Malidarreh N, Ghaseminejad V, Asgari A. Seismic resilience assessment of RC superstructures on long–short combined piled raft foundations: 3D SSI modeling with pounding effects. Structures 2025;81:110176. https://doi.org/10.1016/J.ISTRUC.2025.110176.
[3] Mata R, Nuñez E, Forcellini D. Seismic resilience of composite moment frames buildings with slender built-up columns. J Build Eng 2025;111:113532. https://doi.org/10.1016/J.JOBE.2025.113532.
[4] Kaltakci MY, Arslan MH, Yavuz G. Effect of internal and external shear wall location on strengthening weak RC frames. Sci Iran 2010;17(4).
[5] Hung CC, Hsiao HJ, Shao Y, Yen CH. A comparative study on the seismic performance of RC beam-column joints retrofitted by ECC, FRP, and concrete jacketing methods. J Build Eng 2023;64:105691. https://doi.org/10.1016/J.JOBE.2022.105691.
[6] Narlitepe F, Kian N, Demir U, Demir C, Ilki A. A novel hybrid thin jacketing method for seismic retrofitting of substandard reinforced concrete columns. Eng Struct 2025;342:120879. https://doi.org/10.1016/J.ENGSTRUCT.2025.120879.
[7] Shalif SAHA, Akın A, Aksoylu C, Arslan MH. Strengthening of shear-critical reinforced concrete T-beams with anchored and non-anchored GFRP fabrics applications. Structures 2022;44. https://doi.org/10.1016/j.istruc.2022.08.044.
[8] Xiao Y, Zhou C, Surahman R, Liu Y, Wang Y. Flexural strengthening of reinforced concrete beams with FRP enveloped steel plate. Eng Struct 2025;335:120409. https://doi.org/10.1016/J.ENGSTRUCT.2025.120409.
[9] Saadatmanesh H, Ehsani MR. RC Beams Strengthened with GFRP Plates. I: Experimental Study. J Struct Eng 1991;117:3417–33. https://doi.org/10.1061/(ASCE)0733-9445(1991)117:11(3417).
[10] Attari N, Amziane S, Chemrouk M. Flexural strengthening of concrete beams using CFRP, GFRP and hybrid FRP sheets. Constr Build Mater 2012;37:746–57. https://doi.org/10.1016/J.CONBUILDMAT.2012.07.052.
[11] Tatar J, Viniarski C, Ishfaq M, Harries KA, Head M. Effect of U-wrap anchors on flexural behavior of reinforced concrete beams flexurally strengthened with externally bonded CFRP Sheets. J Compos Constr 2023;27:04022099. https://doi.org/10.1061/JCCOF2.CCENG-3924.
[12] Madotto R, Van Engelen NC, Das S, Russo G, Pauletta M. Shear and flexural strengthening of RC beams using BFRP fabrics. Eng Struct 2021;229:111606. https://doi.org/10.1016/J.ENGSTRUCT.2020.111606.
[13] Zhang S, Wu B. Effects of salt solution on the mechanical behavior of concrete beams externally strengthened with AFRP. Constr Build Mater 2019;229:117044. https://doi.org/10.1016/J.CONBUILDMAT.2019.117044.
[14] Rageh BO, El-Mandouh MA, Elmasry AH, Attia MM. Flexural Behavior of RC beams strengthened with gfrp laminate and retrofitting with novelty of adhesive material. Buildings 2022;12:1444. https://doi.org/10.3390/BUILDINGS12091444.
[15] Triantafillou TC. Shear strengthening of reinforced concrete beams using epoxy-bonded FRP composites. Struct J 1998;95:107–15. https://doi.org/10.14359/531.
[16] Barros JAO, Dias SJE, Lima JLT. Efficacy of CFRP-based techniques for the flexural and shear strengthening of concrete beams. Cem Concr Compos 2007;29:203–17. https://doi.org/10.1016/J.CEMCONCOMP.2006.09.001.
[17] Oz I. Resilience of hospital structures under seismic loads: A case study informed by the 2023 Maraş earthquake. Structures 2025;74:108642. https://doi.org/10.1016/J.ISTRUC.2025.108642.
[18] Kameshwar S, Forcellini D, Barbosa AR. Assessment of building recovery functions for local and global resilience assessment to tsunamis. Resilient Cities Struct 2025;4:132–45. https://doi.org/10.1016/J.RCNS.2025.10.001.
[19] Hoseny ME, Forcellini D, Ma J. The role of the foundation gap on the pounding between low-rise buildings. Structures 2024;63. https://doi.org/10.1016/j.istruc.2024.106412.
[20] Shariati A, Bayrami SS, Ebrahimi F, Toghroli A. Wave propagation analysis of electro-rheological fluid-filled sandwich composite beam. Mech Based Des Struct Mach 2022;50:1481–90. https://doi.org/10.1080/15397734.2020.1745646.
[21] Shariati A, Qaderi S, Ebrahimi F, Toghroli A. On buckling characteristics of polymer composite plates reinforced with graphene platelets. Eng Comput 2022;38:513–24. https://doi.org/10.1007/S00366-020-00992-2.
[22] Szinyéri B, Kővári B, Völgyi I, Kollár D, Joó AL. A strain gauge-based Bridge Weigh-In-Motion system using deep learning. Eng Struct 2023;277:115472. https://doi.org/10.1016/J.ENGSTRUCT.2022.115472.
[23] Alsuhaibani E. Optimization of Carbon Fiber-Reinforced Polymer (CFRP) configuration for enhanced flexural performance in strengthened concrete beams. Buildings 2024;14:3953. https://doi.org/10.3390/BUILDINGS14123953.
[24] Haddad RH, Marji CS. Composite Strips with U-Shaped CFRP wrap anchor systems for strengthening reinforced concrete beams. Int J Civ Eng 2019;17:1799–811. https://doi.org/10.1007/S40999-019-00447-W.
[25] Mhanna HH, Hawileh RA, Abdalla JA. Shear strengthening of reinforced concrete beams using CFRP Wraps. Procedia Struct Integr 2019;17:214–21. https://doi.org/10.1016/J.PROSTR.2019.08.029.
[26] Aksoylu C. Shear strengthening of reinforced concrete beams with minimum CFRP and GFRP strips using different wrapping technics without anchoring application. Steel and Composite Structures. Int J 2022;44:845–65. https://doi.org/10.12989/scs.2022.44.6.845.
[27] Mostofinejad D, Hosseini SA, Razavi SB. Influence of different bonding and wrapping techniques on performance of beams strengthened in shear using CFRP reinforcement. Constr Build Mater 2016;116:310–20. https://doi.org/10.1016/J.CONBUILDMAT.2016.04.113.
[28] Cao VVan. Effects of CFRP U-Wraps on the Behavior of NSM GFRP retrofitted reinforced concrete beams. J Compos Constr 2025;29:04024087. https://doi.org/10.1061/JCCOF2.CCENG-4884.
[29] Mhanna HH, Hawileh RA, Abdalla JA. Comparative analysis of design guidelines for FRP contribution to shear capacity of strengthened RC beams. Procedia Struct Integr 2022;37:359–66. https://doi.org/10.1016/J.PROSTR.2022.01.096.
[30] Baggio D, Soudki K, Noël M. Strengthening of shear critical RC beams with various FRP systems. Constr Build Mater 2014;66:634–44. https://doi.org/10.1016/J.CONBUILDMAT.2014.05.097.
[31] Mofidi A, Chaallal O. Shear Strengthening of RC Beams with Externally Bonded FRP Composites: Effect of Strip-Width-to-Strip-Spacing Ratio. J Compos Constr 2011;15:732–42. https://doi.org/10.1061/(ASCE)CC.1943-5614.0000219.
[32] Subramaniam KV, Carloni C, Nobile L. Width effect in the interface fracture during shear debonding of FRP sheets from concrete. Eng Fract Mech 2007;74:578–94. https://doi.org/10.1016/J.ENGFRACMECH.2006.09.002.
[33] Tang Y, Wang W, Huang Q, Cheng Y, Zhou C. Shear performance prediction of RC beams shear-strengthened with FRP sheet: a machine learning driven design-oriented method. Eng Struct 2025;334:120240. https://doi.org/10.1016/J.ENGSTRUCT.2025.120240.
[34] Täljsten B. Strengthening concrete beams for shear with CFRP sheets. Constr Build Mater 2003;17:15–26. https://doi.org/10.1016/S0950-0618(02)00088-0.
[35] Maalej M, Leong KS. Effect of beam size and FRP thickness on interfacial shear stress concentration and failure mode of FRP-strengthened beams. Compos Sci Technol 2005;65:1148–58. https://doi.org/10.1016/J.COMPSCITECH.2004.11.010.
[36] Li LJ, Guo YC, Liu F, Bungey JH. An experimental and numerical study of the effect of thickness and length of CFRP on performance of repaired reinforced concrete beams. Constr Build Mater 2006;20:901–9. https://doi.org/10.1016/J.CONBUILDMAT.2005.06.020.
[37] Jin L, Xia H, Jiang X ang, Du X. Size effect on shear failure of CFRP-strengthened concrete beams without web reinforcement: Meso-scale simulation and formulation. Compos Struct 2020;236:111895. https://doi.org/10.1016/J.COMPSTRUCT.2020.111895.
[38] Jin L, Zhang J, Li D, Du X. Meso-scale analysis of shear performance and size effect of CFRP sheets strengthened RC beams. Structures 2022;45:1630–45. https://doi.org/10.1016/J.ISTRUC.2022.09.104.
[39] Guo H, Liao HH, Su M, Zhang B, Li S, Peng H. Shear strengthening of RC beams with prestressed NSM CFRP: Influencing factors and analytical model. Compos Struct 2024;342:118262. https://doi.org/10.1016/J.COMPSTRUCT.2024.118262.
[40] Jin L, Qin P, Zhang J, Li D, Jiang X ang, Du X. Size effect in shear failure of RC beams reinforced with CFRP sheets: Influences of CFRP adhesion angle and shear-span ratio. Eng Struct 2025;326:119543. https://doi.org/10.1016/J.ENGSTRUCT.2024.119543.
[41] Alhassan MA, Al-Rousan RZ, Alomari IS, Amaireh L. Shear response of RC beams encompassing hybrid CFRP strips and steel stirrups: Beam depth effect. Structures 2022;38:781–96. https://doi.org/10.1016/J.ISTRUC.2022.02.043.
[42] Alsayed SH, Siddiqui NA. Reliability of shear-deficient RC beams strengthened with CFRP-strips. Constr Build Mater 2013;42:238–47. https://doi.org/10.1016/J.CONBUILDMAT.2013.01.024.
[43] Lima MM, Doh JH, Hadi MNS, Miller D. The effects of CFRP orientation on the strengthening of reinforced concrete structures. Struct Des Tall Spec Build 2016;25:759–84. https://doi.org/10.1002/tal.1282.
[44] Arslan MH, Yazman Ş, Hamad AA, Aksoylu C, Özkılıç YO, Gemi L. Shear strengthening of reinforced concrete T-beams with anchored and non-anchored

CFRP fabrics. Structures 2022;39:527–42. https://doi.org/10.1016/J.ISTRUC.2022.03.046.
[45] Duo Y, Ma M, Xu G, Liu X. Effect of adhesive on the anchorage performance of variable curvature waveform clamping anchor for CFRP plate: Experimental investigation and carrying capacity calculation. Case Stud Constr Mater 2025;22:e04322. https://doi.org/10.1016/J.CSCM.2025.E04322.
[46] Zhou J, Wang X, Liu X, Shi J, Huang H, Li Y, et al. Numerical and experimental evaluation of a variable-stiffness wedge anchorage for basalt-fiber-reinforced polymer tendons. Eng Struct 2024;304:117684. https://doi.org/10.1016/J.ENGSTRUCT.2024.117684.
[47] Shi J, Wang X, Zhang L, Wu Z, Zhu Z. Composite-wedge anchorage for fiber-reinforced polymer tendons. J Compos Constr 2022;26. https://doi.org/10.1061/(ASCE)CC.1943-5614.0001194.
[48] Niu Y, Xian G, Guo R. Design and service performance of FRP anchorage system: A review. Rev Mater Res 2025;1:100038. https://doi.org/10.1016/J.REVMAT.2025.100038.
[49] Zaki MA, Rasheed HA, Roukerd RR, Raheem M. Performance of reinforced concrete T beams strengthened with flexural CFRP sheets and secured using CFRP splay anchors. Eng Struct 2020;210:110304. https://doi.org/10.1016/J.ENGSTRUCT.2020.110304.
[50] Saeed YM, Aules WA, Rad FN, Raad AM. Tensile behavior of FRP anchors made from CFRP ropes epoxy-bonded to uncracked concrete for flexural strengthening of RC columns. Case Stud Constr Mater 2020;13:e00435. https://doi.org/10.1016/J.CSCM.2020.E00435.
[51] Shan B, Pan Y, Huo X, Xian G. Detection of slip for CFRP-concrete interface using stereovision method corrected by epipolar constraint. Struct Control Health Monit 2018;25:e2212. https://doi.org/10.1002/stc.2212.
[52] Alam MA, Al Riyami K. Shear strengthening of reinforced concrete beam using natural fibre reinforced polymer laminates. Constr Build Mater 2018;162:683–96. https://doi.org/10.1016/J.CONBUILDMAT.2017.12.011.
[53] Tran H, Nguyen-Thoi T, Dinh HB. State-of-the-art review of studies on the flexural behavior and design of FRP-reinforced concrete beams. 2025;18:3295 Materials 2025;18:3295. https://doi.org/10.3390/MA18143295.
[54] Brunner AJ. Quantification of delamination resistance data of FRP composites and its limits. Proc Inst Mech Eng Part L J Mater Des Appl 2025;239:694–705. https://doi.org/10.1177/14644207241280372.
[55] Tran CTN, Nguyen XH, Nguyen HC, Le DD. Shear performance of short-span FRP-reinforced concrete beams strengthened with CFRP and TRC. Eng Struct 2021;242:112548. https://doi.org/10.1016/J.ENGSTRUCT.2021.112548.
[56] Li W, Leung CKY. Effect of shear span-depth ratio on mechanical performance of RC beams strengthened in shear with U-wrapping FRP strips. Compos Struct 2017;177:141–57. https://doi.org/10.1016/J.COMPSTRUCT.2017.06.059.
[57] Li W, Leung CKY. Shear Span–Depth Ratio Effect on Behavior of RC Beam Shear Strengthened with Full-Wrapping FRP Strip. J Compos Constr 2015;20:04015067. https://doi.org/10.1061/(ASCE)CC.1943-5614.0000627.
[58] Al-Saawani MA, El-Sayed AK, Al-Negheimish AI. Effect of shear-span/depth ratio on debonding failures of FRP-strengthened RC beams. J Build Eng 2020;32:101771. https://doi.org/10.1016/J.JOBE.2020.101771.
[59] Mei SJ, Bai YL, Dai JG. Shear strengthening of reinforced concrete beams completely wrapped by large rupture strain (LRS) FRP. Eng Struct 2024;314:118361. https://doi.org/10.1016/J.ENGSTRUCT.2024.118361.
[60] Song B, Jin L, Zhang J, Du X. Size effect tests on shear strength of Basalt FRP-RC deep beams with different shear-span ratios. Eng Struct 2023;294:116740. https://doi.org/10.1016/J.ENGSTRUCT.2023.116740.
[61] Azhar S, Sugiman S, Omar Z, Ahmad H. Experimental investigations of strengthened beam with co-cured carbon FRP and mussel shell-modified epoxy. Ain Shams Eng J 2025;16:103563. https://doi.org/10.1016/J.ASEJ.2025.103563.
[62] Rashid K, Fatima M, Daud M, Ju M, Wang Y. Pull-off capacity of FRP–concrete composite bonded with epoxy/geopolymer at elevated temperature. Struct Concr 2024;25:1241–56. https://doi.org/10.1002/SUCO.202300210.
[63] Raza A, Elhag AB, Ouni MH, El, Arshad M. Effectiveness of FRP confinement for low strength recycled aggregate concrete compressive members having optimized combination of fibers. Struct Concr 2024;25:1092–104. https://doi.org/10.1002/SUCO.202300310.
[64] Ranolia KV, Thakkar BK, Rathod JD. Effect of different patterns and cracking in FRP wrapping on compressive strength of confined concrete. Procedia Eng 2013;51:169–75. https://doi.org/10.1016/J.PROENG.2013.01.025.
[65] Ahmed M, Colajanni P, Pagnotta S. Influence of cross-section shape and FRP reinforcement layout on shear capacity of strengthened RC Beams. 2022;15:4545 Materials 2022;15:4545. https://doi.org/10.3390/MA15134545.
[66] Nguyen-Minh L, Phan-Vu P, Tran-Thanh D, Phuong Thi Truong Q, Pham TM, Ngo-Huu C, et al. Flexural-strengthening efficiency of cfrp sheets for unbonded post-tensioned concrete T-beams. Eng Struct 2018;166:1–15. https://doi.org/10.1016/J.ENGSTRUCT.2018.03.065.
[67] Li Y, Chen H, Yi WJ, Peng F, Li Z, Zhou Y. Effect of member depth and concrete strength on shear strength of RC deep beams without transverse reinforcement. Eng Struct 2021;241:112427. https://doi.org/10.1016/J.ENGSTRUCT.2021.112427.
[68] Wang G, Gu L, Nie J, Qu T, Wu C, Zhang Y, et al. Shear strengthening of full-scale RC beams with externally bonded ultra-high performance concrete (UHPC) plates with embedded CFRP strips. Case Stud Constr Mater 2025;22:e04851. https://doi.org/10.1016/J.CSCM.2025.E04851.
[69] Wang JJ, Zhang SS. Design-oriented stress–strain model for fiber-reinforced polymer (FRP)-confined ultra-high-performance concrete (UHPC). Compos Struct 2025;357:118893. https://doi.org/10.1016/J.COMPSTRUCT.2025.118893.
[70] Chen B, Zhou J, Zhang D, Su J, Nuti C, Sennah K. Experimental study on shear performances of ultra-high performance concrete deep beams. Structures 2022;39:310–22. https://doi.org/10.1016/J.ISTRUC.2022.03.019.
[71] Al-Tersawy SH. Effect of fiber parameters and concrete strength on shear behavior of strengthened RC beams. Constr Build Mater 2013;44:15–24. https://doi.org/10.1016/J.CONBUILDMAT.2013.03.007.
[72] Ministry of Environment and Urbanization. Turkish building earthquake code (TBEC-2018). Ankara, Turkey: 2018.
[73] American Concrete Institute. ACI 440.2R-17: Guide for the Design and Construction of Externally Bonded FRP Systems for Strengthening Concrete Structures. Farmington Hills, MI: 2017.
[74] Fédération Internationale du Béton (FIB). fib Model Code for Concrete Structures 2010. Ernst & Sohn, Wiley; 2013.
[75] CNR – National Research Council of Italy. Guidelines for the Design and Construction of Structural Strengthening Interventions Using Externally Bonded FRP Systems. Rome, Italy: CNR; 2013.
[76] Turkish Standards Institution. Building code requirements for reinforced concrete (TS 500). Ankara, Turkey: 2000.
[77] European Committee for Standardization (CEN). Testing Hardened Concrete – Part 3: Compressive Strength of Test Specimens (EN 12390–3). Brussels, Belgium: 2019.
[78] European Committee for Standardization (CEN). Steel for the Reinforcement and Prestressing of Concrete – Test Methods – Part 1: Reinforcing Bars, Rods and Wire (EN ISO 15630–1). Brussels, Belgium: 2019.
[79] European Committee for Standardization (CEN). Metallic Materials – Tensile Testing – Part 1: Method of Test at Room Temperature (EN ISO 6892–1). Brussels, Belgium: 2019.
[80] Kalfas KN, Ghorbani Amirabad N, Forcellini D. The role of shear modulus on the mechanical behavior of elastomeric bearings when subjected to combined axial and shear loads. Eng Struct 2021;248:113248. https://doi.org/10.1016/J.ENGSTRUCT.2021.113248.
[81] Davoodnabi SM, Mirhosseini SM, Shariati M. Analyzing shear strength of steel-concrete composite beam with angle connectors at elevated temperature using finite element method. Steel Compos Struct 2021;40:853. https://doi.org/10.12989/SCS.2021.40.6.853.
[82] Chen JF, Teng JG. Shear capacity of FRP-strengthened RC beams: FRP debonding. Constr Build Mater 2003;17:27–41. https://doi.org/10.1016/S0950-0618(02)00091-0.
[83] Mukhtar F, Jawdhari A. RC beams flexurally strengthened with CFRP sheets combined with FRC layer for mitigating debonding failures. Constr Build Mater 2024;427:136274. https://doi.org/10.1016/J.CONBUILDMAT.2024.136274.
[84] Shariati M, Grayeli M, Shariati A, Naghipour M. Performance of composite frame consisting of steel beams and concrete filled tubes under fire loading. Steel Compos Struct 2020;36:587. https://doi.org/10.12989/SCS.2020.36.5.587.
[85] Grace NF, Soliman AK, Abdel-Sayed G, Saleh KR. Behavior and Ductility of Simple and Continuous FRP Reinforced Beams. J Compos Constr 1998;2:186–94. https://doi.org/10.1061/(ASCE)1090-0268(1998)2:4(186).
[86] Zhang X, Hao J, Hou W, Yao J, Wang Y, Su X, et al. Debonding analysis of frp-strengthened concrete beam in high-temperature environment: an enhanced understanding on sustainable structure. 2024;14:4079 Buildings 2024;14:4079. https://doi.org/10.3390/BUILDINGS14124079.
[87] Shariati M, Raeispour M, Naghipour M, Kamyab H, Memarzadeh A, Nematzadeh M, et al. Flexural behavior analysis of double honeycomb steel composite encased concrete beams: an integrated experimental and finite element study. Case Stud Constr Mater 2024;20:e03299. https://doi.org/10.1016/J.CSCM.2024.E03299.